정 미 원 교수지도

석사학위 청구논문

Al_2O_3, Y_2O_3기 복합 무기금속산화물의 합성과 수소투과 특성 평가

2013

성신여자대학교 대학원

화학과

손 보 영

Al_2O_3, Y_2O_3기 복합 무기금속산화물의 합성과 수소투과 특성 평가

정 미 원 교수지도

이 논문을 석사학위논문으로 제출함.

2012년 11월

성신여자대학교 대학원

화학과

손 보 영

인 준 서

손보영의 석사학위 논문으로 인준함.

심사위원 인

심사위원 인

심사위원 인

성신여자대학교 대학원

논 문 개 요

저온에서 합성이 가능하고 합성과정이 용이하며 고순도 재료를 제조할 수 있는 졸-겔 법을 이용하여 열적 및 화학적으로 안정한 다공성 세라믹 재료로 복합산화물을 합성하였다. 비표면적을 증가시키기 위해 킬레이트 효과를 볼 수 있는 옥살산을 첨가하였다. 수소분리막의 제조는 디스크 타입의 펠렛으로 성형하여 이용하였으며 이 분리막을 사용하기 위해서는 내구성이 필요하다. 기계적 강도가 크고 연성을 가지는 니켈 금속 분말을 이용하여 두 분말 재료를 기계적 합금화법으로 혼합하고, 열간 압축 성형법을 이용하여 세라믹/금속 복합재료 분리막을 제조하였다. 하지만 이 복합재료 분리막은 수소 분리 실험 시 어느 정도의 압력을 가했을 때 금이 가는 단점이 있다. 이 단점을 보완하기 위해 실리콘 카바이드 슬러지 분말을 이용하였다. 실리콘 카바이드 분말은 내구성이 뛰어나며 슬러지를 재활용한다는 점에서 친환경적인 실험이다. 합성한 분말과 제조한 분리막은 TG-DTA, XRD, FE-SEM, BET 를 이용하여 특성 평가를 진행하였고 분리막을 이용한 수소 투과 특성평가는 다양한 압력과 온도 하에서 수소 가스를 이용하여 진행하였다.

Contents

LIST OF TABLES

LIST OF FIGURES

Ⅰ. Introduction

The hydrogen separation process is one of the technologies that needed for preparing future hydrogen energy system. There are main technologies available for H_2 separation, pressure swing adsorption (PSA), cryogenic distillation and selective permeation through a membrane [1]. Membrane separation has the advantage over other separation methods in that it is simple and potentially less energy intensive. H_2 separation membranes can be classified into four categories; dense metal, nano-porous inorganic materials, organic polymers and dense ion transport membranes based on proton conducting materials [2].

Hydrogen separation membranes have developed from various materials, such as palladium and its alloys. Xomeritakis et al. prepared Pd and Pd/Ag membranes to improve the stability of Pd membranes but there are still some problems in their stability at high temperature and pressure. Ceramic membranes have been developed for hydrogen generation, separation and purification through the reforming process. They are known to be membrane materials to maintain high stability at high temperatures [3-4]. Ceramic-metal (cermet) composite membranes with high permeability and selectivity have been interested in numerous area, such as hydrogen purification, fuel cell technology and membrane reactor processes. The permeance is defined as $F=Q/S(P_h-P_l)$ with Q being the molar gas flow rate, S the permeation area of the membrane, and P_h and P_l the pressures upstream and downstream, respectively [5-7].

Microporous membrane are usually inorganic membranes with pore sizes smaller than 2 nm and are composed mainly of either amorphous silica, carbon or zeolites. A microporous ceramic membrane system generally consists of a macroporous ceramic support, some ceramic intermediate layers, and eventually a highly selective top layer. The support provides mechanical strength to the system. The intermediate layers bridge the gap between the large pores of the support and the small pores of the top layer. The top layer has separating capacities. Membrane properties such as permeation and selectivity depend on the microstructures of the membrane/support composites such as pore size and distribution, porosity and the affinity between permeating species and the pore walls. Separation of a gas mixture can take place based on differences in molecular mass, size or shape, or on differences in the affinity of the gas molecules to the membrane material. Selectivity is generally increased along with decrease of pore size and overall porosity of the membrane [8-11].

Alumina can be transformed by changing the temperature via the boehmite$\Rightarrow \gamma \Rightarrow \delta \Rightarrow \theta \Rightarrow \alpha$ phases and different phases can be obtained depending on the processes used. Mesoporous γ-Al_2O_3 is usually prepared by heating to 673~773 K from boehmite. γ-Al_2O_3 among the transition phases of alumina has especially remarkable textural and acid-base properties; therefore, it has been used as a type of ceramic support and as a heterogeneous catalyst [12-14]. Moreover, it has the potential for broad

application as an adsorbent catalyst, a catalytic support and an advanced ceramic owing to the thermal and chemical stability of its optical characteristics. Alumina, based on its fine particle size, high surface area and good catalytic activity, has a great potential for several applications, such as an adsorbent, coating material, ceramic membrane, catalyst and its support. In order to improve the stability of membrane, metal oxide such as TiO_2, ZrO_2, NiO, etc can be added to alumina and also the stability of these membranes at higher temperatures is able to be enhanced [8-9], so it makes improving thermal stability and the surface area. NiO is also considered as a catalyst because it is highly active and selective not only in hydrogenation but also catalytic reactions. It is used as a supporting co-catalyst with ceramic substrates such as silica and alumina [15-19]. NiO doping to Al_2O_3 powder can be prepared by several techniques. Especially, the sol-gel process can change the microstructure of homogeneous inorganic material precisely with controlling size and morphology of condensation materials [20-25].

Sol-gel method enables to make of high purity ceramic materials with homogeneous distribution at low temperatures compared with other synthetic routes such as chemical vapor deposition (CVD) and hydrothermal method. Oxalic acid could play a role as a chelate holding on the mixed ions and controller for making the moderate pore size. Recent study was reported that oxalic acid could forma mixed precursor, which acts as a substrate for the homogeneous distribution of the mixed metal oxide phases

[26-30].

Transparent poly-crystalline yttria has been considered as important ceramic material owing to its excellent optical and refractory characteristics. It is found uses as a chemically and thermally stable substrate, crucible material for melting reactive metals, and nozzle material for jet casting molten rare earth - iron magnetic alloys. High specific area and thermal stability are the major requirements for porous ceramic membrane. Y_2O_3 has been applied in a wide range of areas because of its optical, thermal and chemical stabilities. Particularly unique physical and chemical properties of Y_2O_3 have been studied for variety of applications in electrochemistry, catalytic chemistry and separation and purification. Yao et al. reported that Y_2O_3 has excellent catalytic reaction of epoxidation [31-38].

CeO_2-based oxide in the membrane has been considered as chemically and thermally stable substrate because it is the major requirement to have a thermal stability for porous ceramic membrane as a gas separation filter [15-16]. $Ce_{0.8}Y_{0.2}O_{1.9}$ ceramics have given much attention as the electrolyte in solid oxide fuel cells. This ceramics show good sintering ability and electrical conductivity due to its higher sintering density and smaller grain size [39-44].

The hydrogen selective SiC membrane has been used for application in membrane reactors for the water gas shift and steam reforming reactions. Silicon carbide as a structural material has advantages because of its excellence of thermal shock with

corrosion resistance at elevated temperatures as well as having low coefficient of thermal expansion and high mechanical strength [45-50]. Due to these advantages, SiC is also suitable for gas and liquid separation filter material.

The purpose of this study is to make hydrogen separation membranes which are highly efficient and economic. At first, we synthesized the 20 wt.% NiO-doped NiO-doped Al_2O_3 powder via sol-gel process and this powder with nickel metal was mixed to make composite membrane by reducing the amount of nickel metal. Nickel is known as good hydrogen dissociation catalyst and the using of inorganic membrane. However there are some disadvantages, such as hydrogen embrittlement and degradation [36-38]. The composite membrane, 20 wt.% NiO-doped Al_2O_3/10 wt.% Ni, was prepared by hot-press sintering and proposed for having their predominant hydrogen permeability and ability to maintain stability and mechanical property at high operating temperatures.

We considered Y_2O_3 as a material of hydrogen permeation membrane next alumina. The advantage of poly-crystalline Y_2O_3 is having a much lower emissivity at high temperatures than Al_2O_3. Also the additive $Ce_{0.8}Y_{0.2}O_{1.9}$ which was made by modified sol-gel method using oxalic acid chelate was selected for the densification of membrane. However, the disadvantage is its mechanical property of hardness which is inversely proportional to the square root of the grain. The hardness can be controlled by reducing the grain size and doping it with other materials,

although it can negatively affect the specific heat capacity and resistance to thermal shock.

To improve the mechanical strength of membrane we prepared dense SiC-based composite membrane as a filter for hydrogen separation keeping the thermal-mechanical stability. Because the addition of these metal oxides with large amounts lead to the degradation of high-temperature stability of SiC ceramics and mismatch between two phases during fabrication of membrane due to different thermal expansion coefficient. SiC ceramic and Y_2O_3 or $Ce_{0.8}Y_{0.2}O_{1.9}$ composite powder was fabricated with Hydrido-polycarbosilane (HPCS) as a binder and then heat-treated at 1173 K under Ar condition.

SiC has various advantages such as thermal-mechanical stability and hardness etc, while SiC has a disadvantage, porous. Thus, SiC+Y_2O_3 composite membrane was prepared with different ratio (Y_2O_3 1, 10, 30 wt.% of SiC), using ball milling and pressure press method to control pore diameter and porosity. The prepared disc membranes passed through dip-coating process (dip-coating, drying and sintering) with Y_2O_3 sol solution to more reduce porosity of SiC. And then the polymer (HPCS) solution was coated onto Y_2O_3 30 wt.% of SiC membrane for top layer of ceramic membrane. In order to enhance the effectiveness of dip-coating, this process was repeated several times.

Ⅱ. Experimental

2.1 Preparation of NiO-doped Al_2O_3/Ni composite membrane

Aluminum isopropoxide ($Al(OC_3H_7)_3$) (CAS No. 555-31-7, Aldrich) was dissolved in distilled water with a mole ratio of $Al(OC_3H_7)_3$:H_2O=1:100 at 353 K. 20 wt.% of $Ni(NO_3)_2 \cdot 6H_2O$ (CAS No. 13478-00-7, Aldrich) with relate to $Al(OC_3H_7)_3$ was added and refluxed for 3 h. 10 wt.% of P123 surfactant was used for the 20 wt.% NiO-doped Al_2O_3 powder with P123. Nitric acid (HNO_3) as an acid catalyst was added to this reaction mixture for peptization to obtain homogeneous sol. This sol solution was stirred overnight and stayed for 24 h to get gel sample after quenching. This gel was washed with water and alcohol, followed by drying at 393 K for 24 h. This powder was heat-treated from 773 K to 1473 K with 200 K interval. To obtain cermet composite membrane for hydrogen permeation test, the mechanical alloying process was done by milling with a zirconia ball for 1h to mix a pure Ni (99.9%, Aldrich) metal and the synthesized powder with P123 obtained after heat-treating at 973 K with a weight ratio of 1:9. The consolidation of powder with nickel metal was performed using hot-press sintering (HPS). The heating rate and the pressure were 5 K/min and 808 MPa. Sintering was proceeded at 1473 K for 2 h under vacuum.

2.2 Preparation of the YCC/Ni composite membrane

Yttrium (Ⅲ) nitrate hexahydrate ($Y(NO_3)_3 \cdot 6H_2O$) (99.8%, CAS No. 13494-98-9, Aldrich) was added to distilled water and the ethanol cosolvent was refluxed at 353K. $Cu(NO_3)_2 \cdot 5H_2O$ (98%, CAS No. 19004-19-4, Aldrich) and $Ce(NO_3)_3 \cdot 6H_2O$ (99%, CAS No. 10294-41-4, Aldrich) were added simultaneously and refluxed for 3h. Nitric acid (HNO_3), a catalyst, and oxalic acid ($C_2H_2O_4$, CAS No. 144-62-7, Aldrich), a chelating agent, were used for the metal Y^{3+} ions involving vigorous stirring and have been adopted to control the rate of hydrolysis. The molar ratio of the metal Y^{3+} ions to oxalic acid was 1:2. The pH was initially adjusted to pH=2±0.1 and remained over night at room temperature. Then, the gel was washed in water several times to remove the ethanol and filtered to eliminate excess solvent. The powder was obtained by drying completed sol at 393 K for 24 h. The obtained powder was heat-treated from 773 K to 1473 K. In order to obtain the membrane specimens for hydrogen permeation, the YCC powders synthesized with oxalic acid were mixed into nano-sized particles using a high energy mill (Fitsch, TH-080).

In order to mix the pure Ni (99.9%, Aldrich) metal and the synthesized powder with oxalic acid heat-treated at 973 K, it was milled with a zirconia ball for 1h during the mechanical alloying process, with a weight ratio of 1:9. The consolidation of the powder was performed using hot-press sintering (HPS). The heating rate and the pressure were 5 K/min and 808 MPa, respectively. Sintering was proceeded at 1473 K for 2 h in a

vacuum. Sievert's type hydrogen permeability equipment was used to measure the hydrogen permeability of YCC/Ni composite membrane. The YCC/Ni composite membrane prepared using the HPS process loaded into the cell and was checked for air leakages. The permeation cell was installed within a heating furnace for temperature control, and the temperature was elevated in a nitrogen atmosphere. To eliminate the oxidation layer that may have formed on the sample surface, it was treated for activation in a hydrogen atmosphere for 1 hour. To avoid cracking the hydrogen separation membrane with thermal shock, the temperature elevation rate was lowered to less than 5 K/min. Also, the cell equipped with the separation membrane was heated. The hydrogen permeability of YCC/Ni composite membrane was measured from RT to 623 K under 0.1~0.3 MPa hydrogen atmosphere.

2.3 Preparation of the $Ce_{0.8}Y_{0.2}O_{1.9}$/SiC composite membrane

$Y(NO_3)_3 \cdot 6H_2O$ (99.8%, Aldrich) and $Ce(NO_3)_3 \cdot 6H_2O$ (99%, Aldrich) were dissolved in distilled water at 353K. Oxalic acid ($C_2H_2O_4$, Aldrich) was added to above solution with vigorous stirring. The pH was initially adjusted to pH=2±0.1 and remained overnight at room temperature. Then, the gel was obtained and washed with water several times. The powder was recovered by drying at 393 K for 24h. This powder was heat-treated from 773 K to 1473 K.

The waste SiC sludge from solar cell industry (BHI CO., LTD) was obtained after centrifugation and magnetism selection process. It is double advantages to reuse waste material as an environment-friendly aspect. This purified SiC ceramic was retreated with HCl, NaOH and washed with H_2O, followed by drying at 373K. This starting SiC ceramic for the SiC-based membrane was analyzed by Rietveld method of XRD results. The amounts of α-phase of SiC-6H, β-phase of SiC-3C and Si were 59.40 %, 35.1 % and 4.5 %, respectively.

For the membrane specimen, purified SiC ceramic and $Ce_{0.8}Y_{0.2}O_{1.9}$ powder (99:1) were mixed using a high energy milling process (Fitsch, TH-080) with the HPCS binder. This mixture was milled with a zirconia ball for 24h for the mechanical alloying process, with a weight ratio of 1:20. These were pressed mechanically at 30 MPa and followed by heat-treatment at 1173 K under Ar gas atmosphere.

Thermal diffusivity of $Ce_{0.8}Y_{0.2}O_{1.9}$/SiC composite membrane was measured and calculated by laser-flash method (Netzsch, lfa-427). To avoid cracking of the membrane by thermal shock, the temperature elevation rate was lowered to less than 5 K/min. The hydrogen permeance of $Ce_{0.8}Y_{0.2}O_{1.9}$/SiC composite membrane was tested on the temperatures at 298, 373, 473, 573 and 673 K under 0.2 MPa by our own permeance experiments at hydrogen atmosphere.

2.4 Preparation of membrane of SiC+Y_2O_3

The waste SiC sludge from solar cell industry (BHI CO., LTD) was obtained after centrifugation and magnetism selection process. It is double advantages to reuse waste material as an environment-friendly aspect. This purified SiC ceramic was retreated with HCl, NaOH and washed with H_2O, followed by drying at 373K. For the membrane specimen, purified SiC ceramic and Y2O3 powder, differing in ratio of Y_2O_3 addition, were mixed using a high energy milling process (Fitsch, TH-080) with the phenol resin as a binder. These were pressed mechanically at 35 MPa into disc pellets of about 14.5 mm diameter and 2 mm thick.

The SiC and Y_2O_3, 1 and 10 wt.%, composite membrane was prepared after heat-treated under Ar condition at 1173 K for 3h. The most important parameters in the dip-coating process were sol concentration, dipping time, ore size and porosity of the support and temperature. The membranes were dipped into the 20ml of above Y_2O_3 sol solution at a constant dipping speed of 0.1 mm/s and kept inside the solution for 5 min. At this point, the viscosity of solution was 25 cP. Then, the dip-coated substrates were kept for drying under air at room temperature for 20 min. After repeating this process for several times, it was heat-treated for 3h at 1173 K.

2.5 Characterization

Thermal degradation of the composites was measured using TG/DTA (NETZSCHSTA 490PC, from room temperature to 1673 K) with a heating rate of 276 K/min under air atmosphere. The crystal structure of the membranes was determined by XRD (X-ray powder diffraction, Bruker D8 Focus with TOPAS). The working voltage of the instrument was 40 kV and the current was 40 mA with Cu Kα (λ = 1.5418Å) radiation. The intensity data was collected at room temperature in a 2θ range from 10° to 80° with a scan rate of 0.2 °/s. The surface morphology of the powders was examined by the JEOL-JMS 7500F FE-SEM operated at 0.5~30 kV. The BET surface area was determined by the adsorption of N_2 with BELSORP-miniⅡ surface area analyzer. The hydrogen permeation equipments were consisted of a pressure controller, mass flow controller (MFC), permeation cell and stainless steel 0.35-inch-long tube that could withstand on high temperature for our experiments. Hydrogen concentration was measured by thermal conductivity detector (TCD) that analyzed the difference between hydrogen and nitrogen gas as carrier through thermal conductivity.

Ⅲ. Results and discussion

3.1 Hydrogen Permeability of NiO-doped Alumina with Nickel Composite Membrane

The TGA and DTA curves of 20 wt.% NiO-doped Al_2O_3 powder with P123 dried at 393 K for 48 h are shown in Fig. 1 (a). The first weight loss around at 473-673 K is because of the evaporation of remaining water and organic group in the reaction mixture. The endothermic peaks until 687.6 K ($\triangle H_{end}$=1.3 kJ/g) are for the phase transformation to the γ-Al_2O_3. The exothermic peak is caused to the rearrangement of aluminum and oxygen ions in the alumina, and another one around from 1073 K to 1373 K was attributed to transformation of γ phase.

Fig. 1 (b) showed XRD patterns of this powder heat-treated at various temperatures. Main peaks of nickel aluminum oxide and with weak peaks of γ-Al_2O_3 start to appear at 773 K. These broad peaks are continued until 1173 K and changed to sharp peaks as increasing temperatures. The γ-Al_2O_3 peaks (JCPDS file No. 50-0741, cubic, a=0.8 nm, S.G=Fd-3m) are observed with the ratio of 3.15% until 1373 K and transformed to α-Al_2O_3 phases (JCPDS file No. 5-0712, Hexagonal, a=0.5 nm, b=0.5 nm, c=1.3 nm) as very sharp peaks with the ratio of 64.66 % at 1473 K. The diffraction peaks of $Ni_{0.94}Al_2O_{3.09}$ (JCPDS file No. 01-078-2180, cubic, a=0.8 nm) are shown with the ratio of 96.85 % and 35.34 % at 1373 K and 1473 K, respectively. They are maintained until 1473 K while peak heights are increased. The surface area with P123 (141.1 m^2/g) were slightly larger than powder without P123

(134.1 m^2/g) because surface area is expected to be improved surface area due to induced hydrogen bonding interaction between non-ionic block copolymer (P123) and Al species.

Fig. 2 showed the XRD pattern for 20 wt.% NiO-doped Al_2O_3/10 wt.% Ni composite membrane (a) before and (b) after hydrogen permeation test. Results showing in both cases are shown the presence of the α-Al_2O_3 (JCPDS file No. 5-0712, Hexagonal, a=0.5 nm, b=0.5 nm, c=1.3 nm), Ni metal (JCPDS file No. 03-1051, cubic, a=0.6 nm) and $NiAl_2O_4$ (JCPDS file No. 10-0339, cubic, a=0.8 nm) with sharp and strong peak intensity. Especially, Ni peak intensity is slightly increased while $NiAl_2O_4$ peaks decreased after hydrogen test. Fig. 3 showed SEM photographs of the surface morphology of the composite membrane (a) before and (b) after hydrogen permeation test, respectively.

The surface of powder before test in Fig. 3 (a) has dense state although the particle sizes are not homogeneous. Nickel metal is spread into pore of the NiO-doped Al_2O_3 powder during the HPS process at high temperature and it gives rise to increase the strength of ceramic-based membrane. Fig. 3 (b) was obtained composite membrane after evaluation of hydrogen permeation. As results of permeation test, it seems to be more porous than before test because hydrogen molecules are passed through grain boundary during the test.

Fig. 4 showed the hydrogen permeation flux of the Al_2O_3-based membrane from room temperature to 673 K under increasing pressure with a range of 1.0, 2.0 and 3.0 bar. These values were

increased with increasing temperature and pressure. The flux for this membrane was obtained as 0.087 mol/m^2s at 473 K. It was better than for the Ni/ceramic membrane ($2.5x10^{-3}$ mol/m^2s at 873 K) [21] and Ni/BCZY cermet membrane ($4.2x10^{-6}$ mol/m^2s at 1173 K) [22]. Reaction enthalpy (⊿H) for the 20 wt.% NiO-doped Al_2O_3/10 wt.% Ni membrane was calculated to 3.7 kJ/mol.

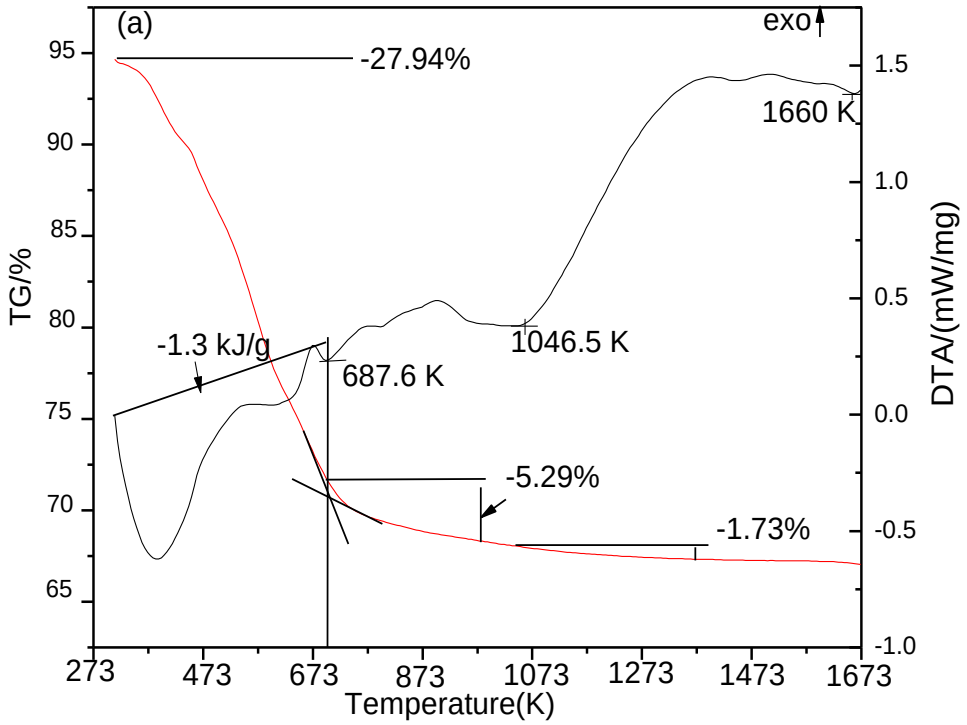
(a)
exo
-27.94%
1660 K
1046.5 K
-1.3 kJ/g
687.6 K
-5.29%
-1.73%
TG/%
DTA/(mW/mg)
Temperature(K)
95
90
85
80
75
70
65
1.5
1.0
0.5
0.0
-0.5
-1.0
273
473
673
873
1073
1273
1473
1673

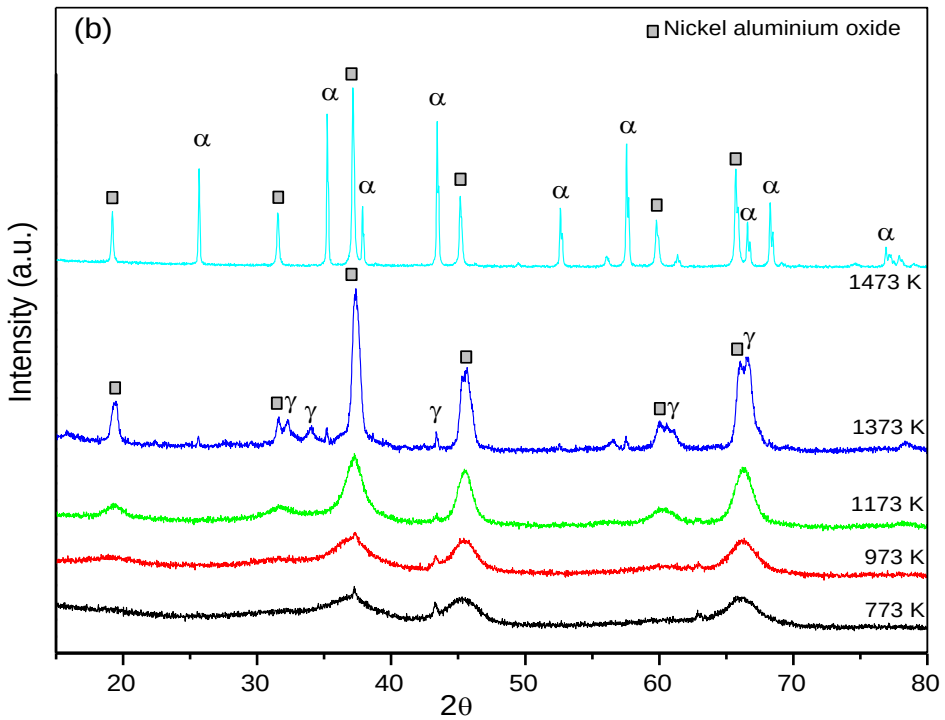

Fig. 1. (a) TG-DTA curves and (b) XRD patterns of the 20 wt.% NiO-doped Al_2O_3 powder with P123.

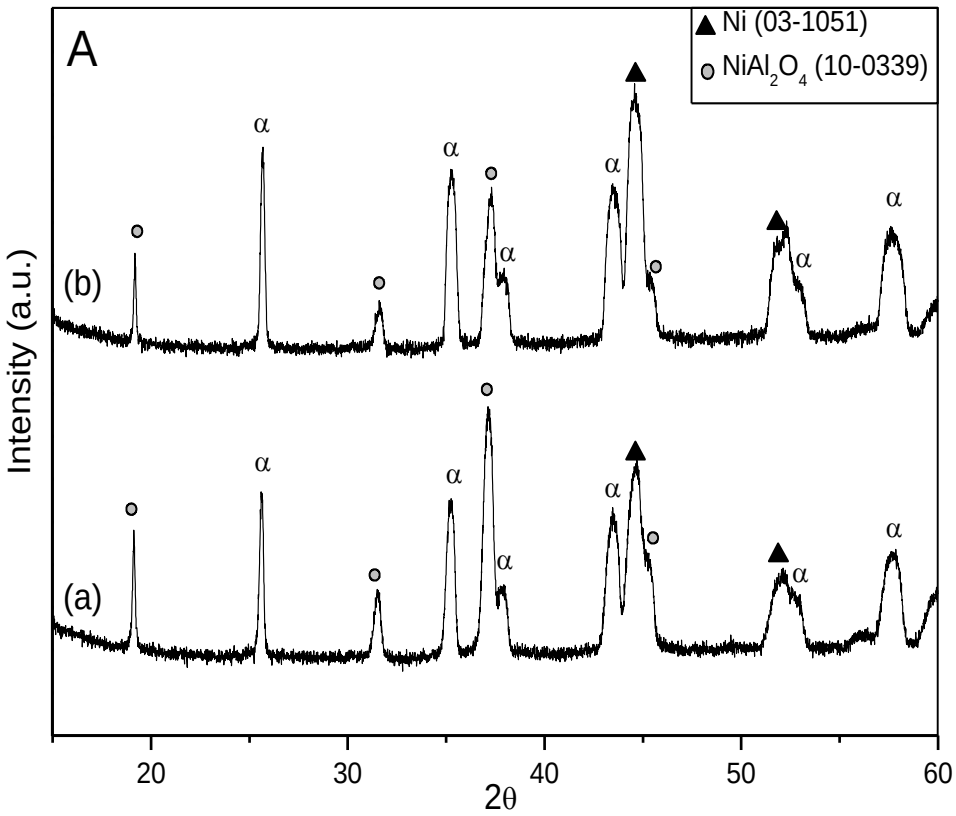

Fig. 2. A. XRD patterns of the 20 wt.% NiO-doped Al_2O_3-10wt% Ni membrane (a) before and (b) after the hydrogen permeation test.

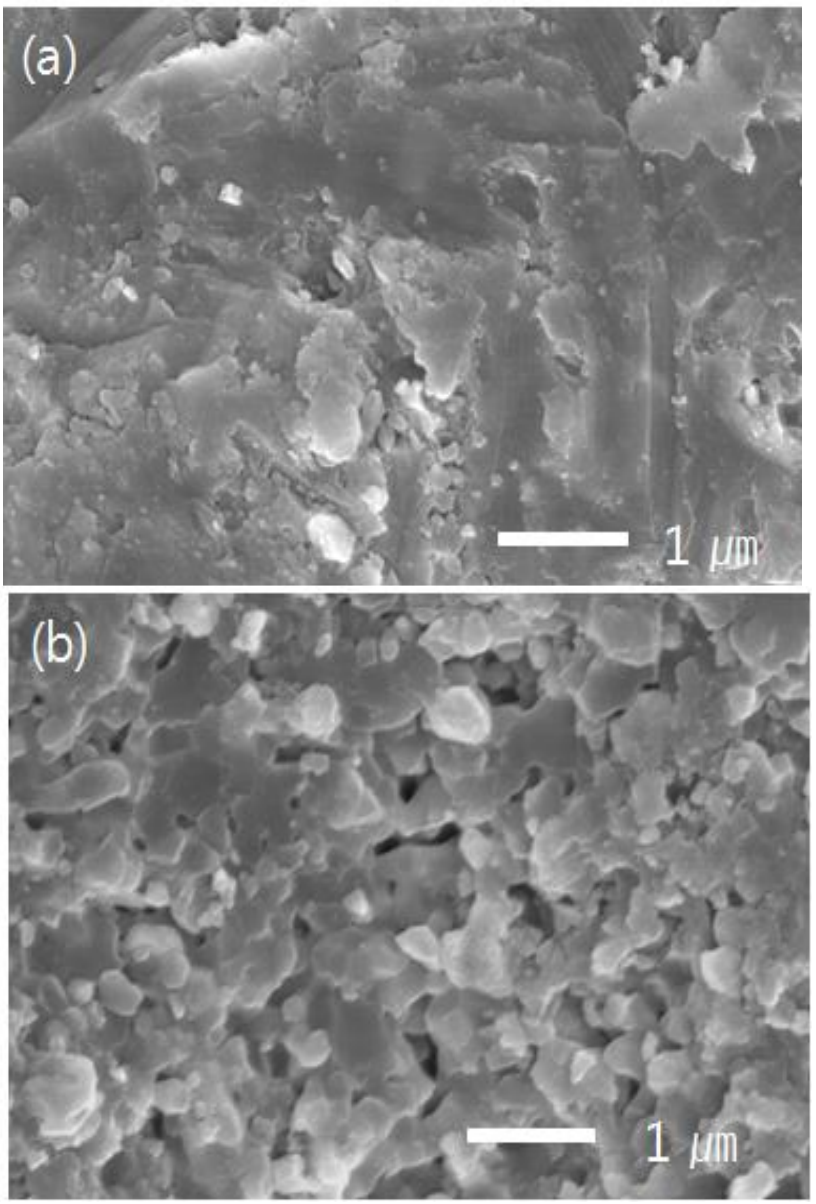

Fig. 3. FE-SEM surface photographs of the 20 wt.% NiO doped Al_2O_3-10 wt.% Ni membrane (a) before and (b) after the hydrogen permeation test.

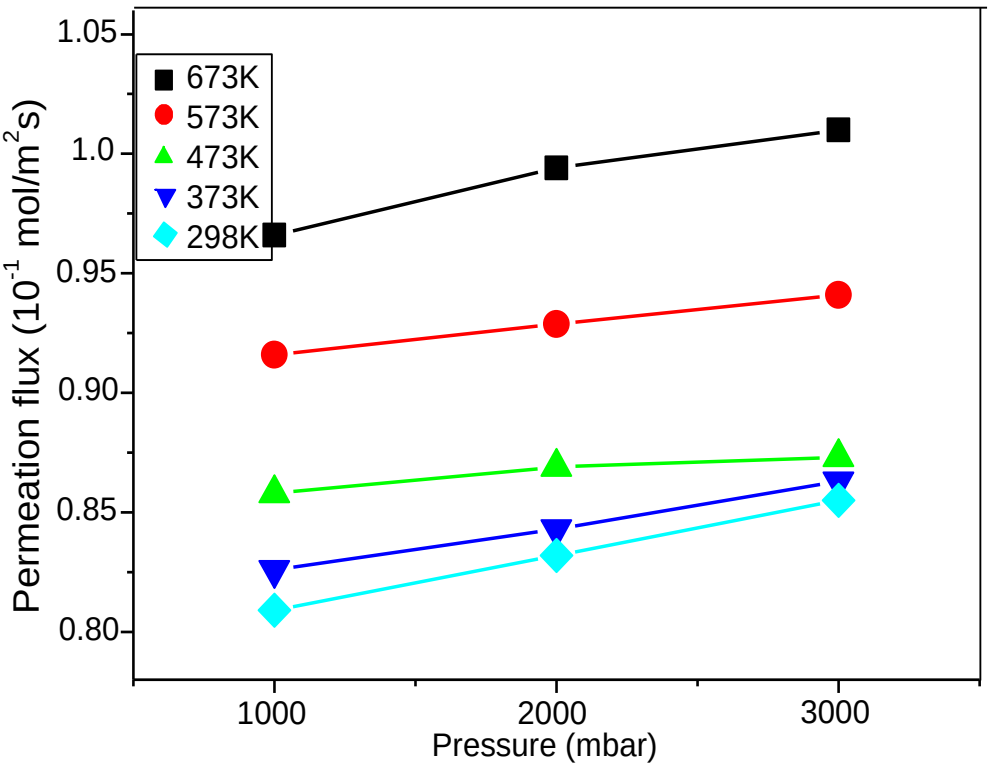

Fig. 4. Hydrogen permeation fluxes through changing pressures on 20 wt.% NiO-doped Al_2O_3/10 wt% Ni membrane.

3.2 Hydrogen permeation of Y_2O_3-CuO-CeO_2/Ni composite membrane

The TG-DTA curves of YCC composite powders with and without oxalic acid was shown in Fig. 5 (a) and (b). The weight loss at 373-673 K was attributed to the dehydration of precursors and the transformation of $Y(OH)_{2.5}(NO_3)_{0.5}$ to Y_2O_3 in Fig. 5 (a). The first step of Fig. 5 (b) was corresponded to the transformation of the precursor gel to dehydrated yttrium oxalate. The thermal decomposition of yttrium oxalate occurred between 573 and 973 K. Especially, yttrium oxalate having a cubic crystal system was produced by the thermal decomposition above 773 K.

Fig. 6 (a) and (b) showed the XRD patterns of heat-treated YCC composite powders with and without oxalic acid at various temperatures. The yttrium oxide peaks having stable cubic structure (JCPDS file No. 41-1105, a=1.0604 nm) were observed above 973 K in Fig. 6 (a) and 773 K in Fig. 6 (b). The peaks of cubic cerium yttrium oxide (JCPDS file No. 01-083-0326, a=1.0757 nm) can be shown above 773 K in Fig. 6 (a), while these were observed at 1173 K in Fig. 6 (b) when synthesized with oxalic acid. Cerium yttrium oxide starts to show up earlier depending on the presence oxalic acid. The reason for the formation of multi-component composites at low temperature might attribute to the chelating agent. Although the direct decomposition of the metal nitrate precursor can produce mesoposous metal oxides, it is difficult to control reaction rate of muti-components. With a further increase of the temperature

from 773 K to 1373 K, the diffraction peaks become sharp and increase in intensity due to the improvement of the crystallinity. The surface morphology and surface area of the YCC composite powder with and without oxalic acid are shown in Fig. 7. Using with oxalic acid, grains have very specific, spherical shapes. FE-SEM measurements at 973 K showed that the grains were related to cerium yttrium oxide from the results of the XRD. The formation of these specific shapes had an impact on the increase of surface area.

Fig. 8 (a) shows nitrogen adsorption isotherms of the YCC composite powder with and without oxalic acid heat-treated at 973 K. Both powders give typical type Ⅳ isotherms with a H_2 hysteresis loop as defined by IUPAC (International Union of Pure and Applied Chemistry). A type N_2 hysteresis loop is commonly associated with ink-bottle pores or voids between close-packed spherical particles. Comparing with both samples, powder with oxalic acid has a higher total pore volume, indicating that pore diameter was mesoporous by analyzing *S*-shape of this diagram. Fig. 8 (b) indicated BJH (Barrett-Joyner-Halenda method) pore size distribution of YCC composite powders. The average pore size was calculated to sharply narrow down from 8.31 to 7.13 nm by adding oxalic acid.

Fig. 9 (a) illustrates the hydrogen permeation flux for YCC 10wt% Ni membrane at 298, 373, 473, 573 and 673 K under increasing pressure with a range of 0.1, 0.2 and 0.3 MPa. The hydrogen flux of this composite membrane was obtained as

$7.7x10^{-7}$ mol/m^2s at 573 K under 0.2 MPa. It was better than for the Pd/YSZ membrane ($4.3x10^{-7}$ mol/m^2s at 873 K). The hydrogen flux increased with increasing pressure but was not correlated with temperature. The membrane has Knudsen diffusion mechanism that is not proportional the increasing temperature and hydrogen pressure. The fig. 9 (b) shows the Arrhenius' s plot for hydrogen permeation data. The calculated data of heat of the process (ΔH) for YCC/10 wt.% Ni membrane was 0.84 kJ/mol. This result shows that hydrogen permeation through membrane was measured with the endothermic reaction and dominated by gas pressure.

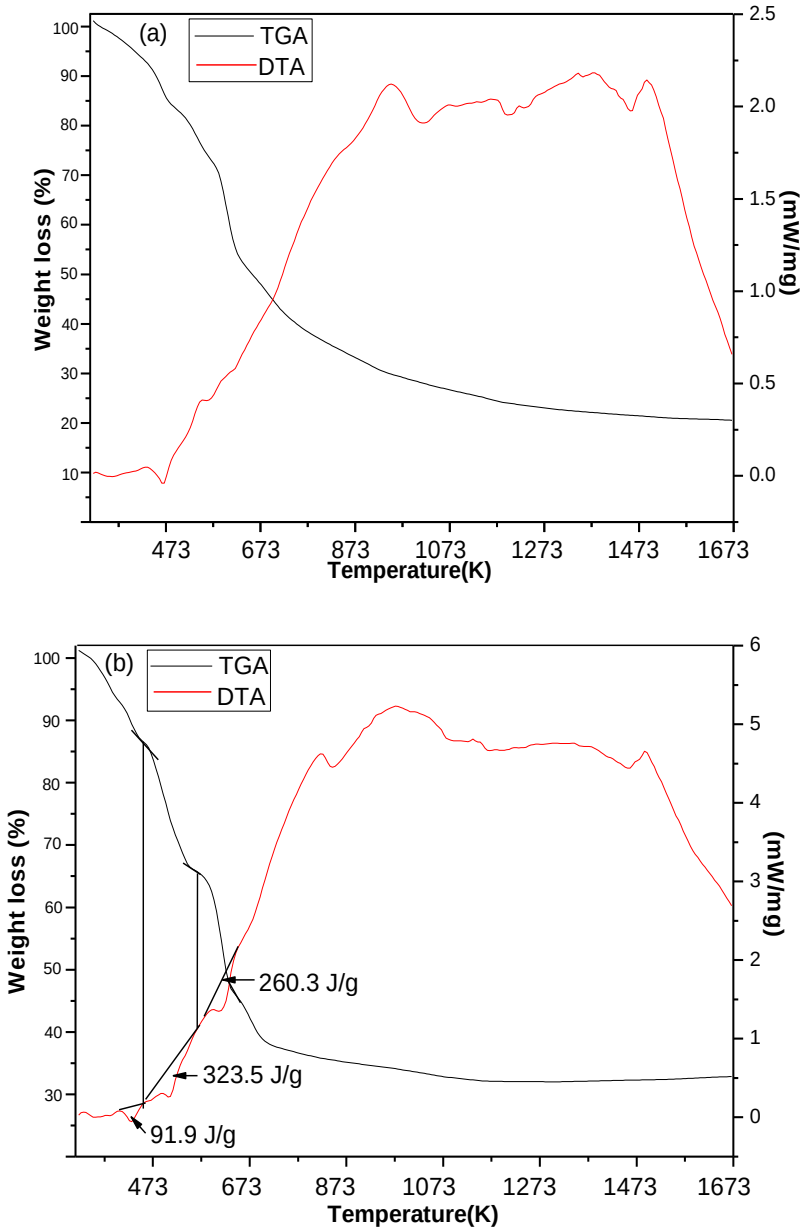

Fig. 5. TG-DTA curves of the YCC powder (a) with (b) without oxalic acid.

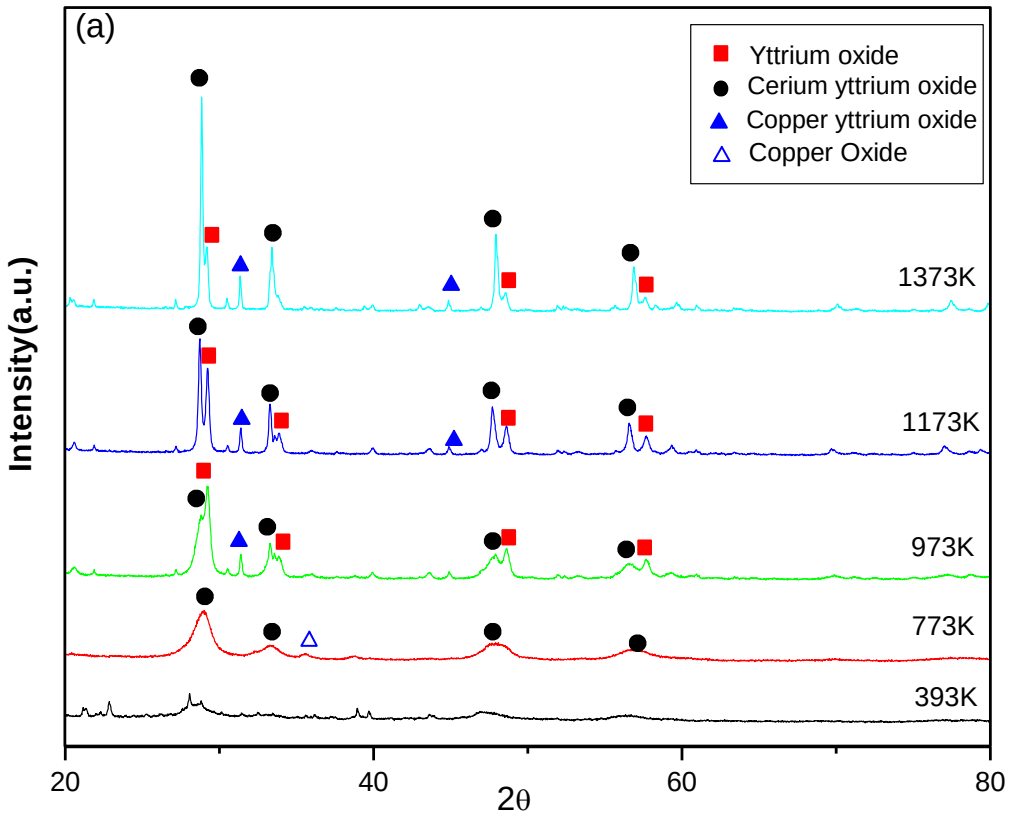
(a)
Yttrium oxide
Cerium yttrium oxide
Copper yttrium oxide
Copper Oxide
1373K
1173K
973K
773K
393K
Intensity(a.u.)
20
40
60
80
2θ

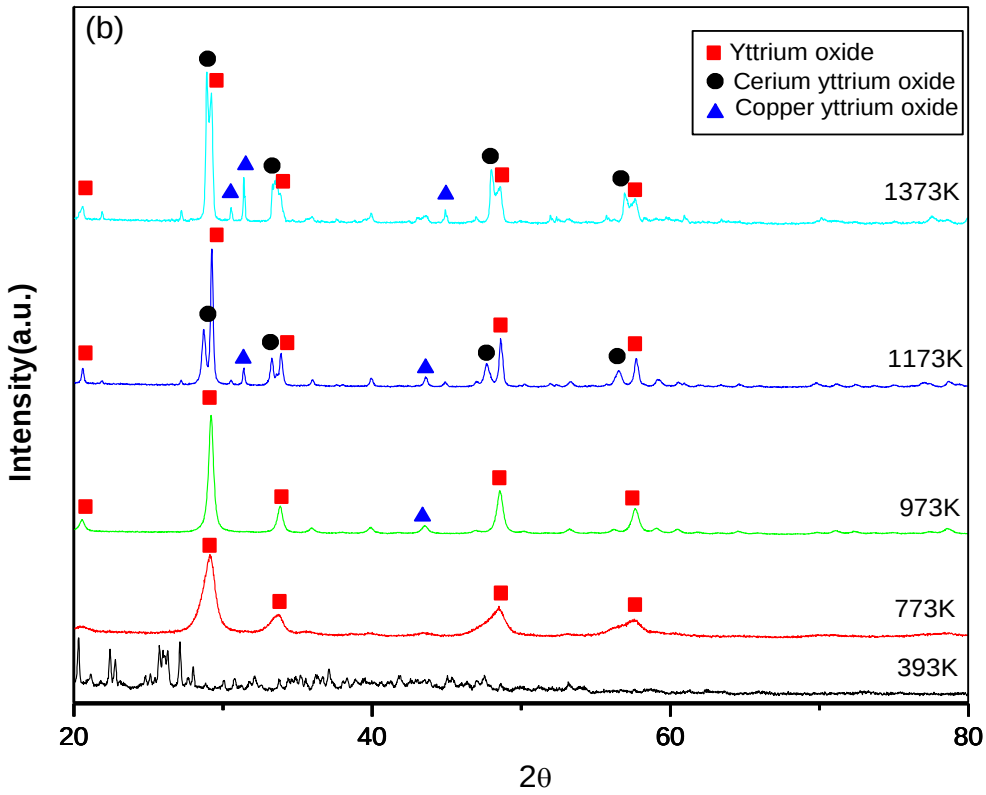

Fig. 6. XRD patterns of the YCC powder (a) with (b) without oxalic acid heat-treated at various temperatures.

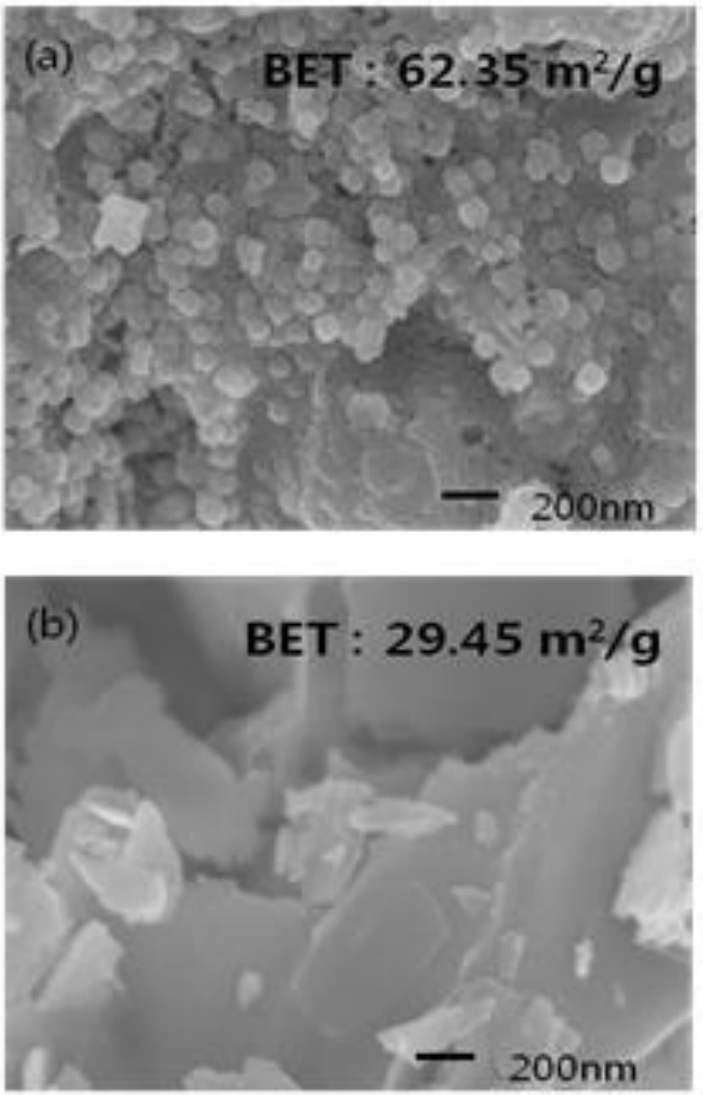

Fig. 7. FE-SEM micrographs and BET result of the YCC powder (a) with (b) without oxalic acid heat-treated at 973 K.

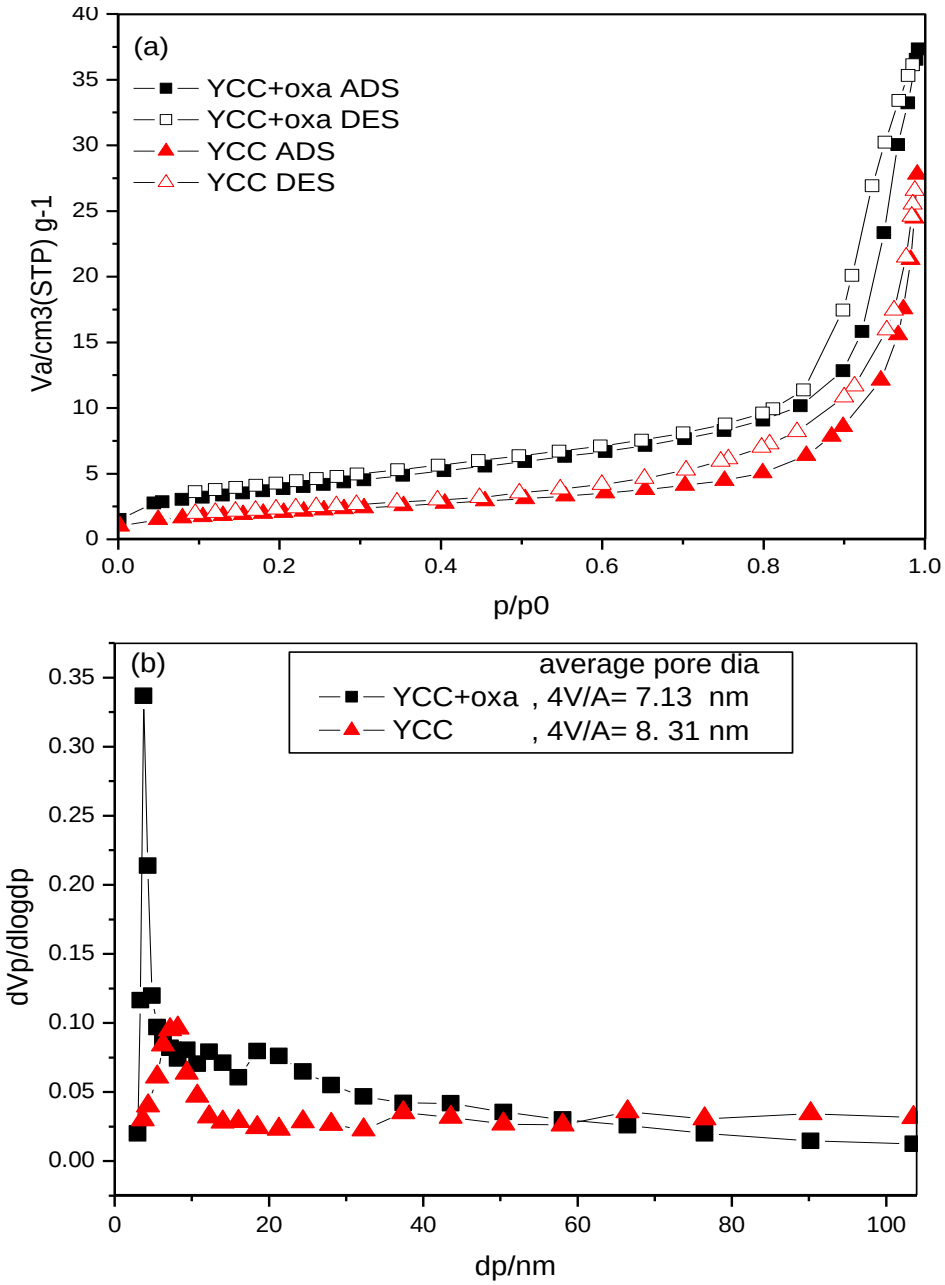

Fig. 8. (a) Nitrogen adsorption-desorption isotherms and (b) pore size distribution of the YCC powders with and without oxalic acid heat-treated at 973 K.

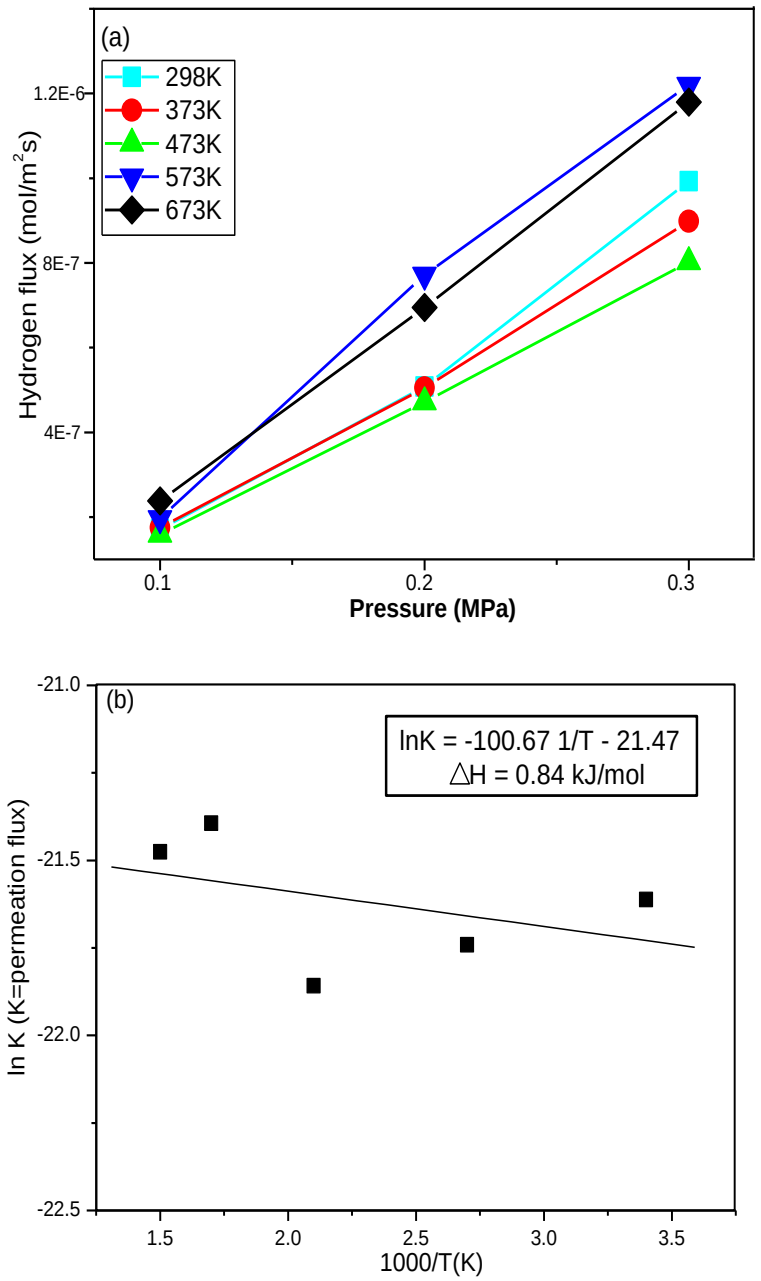

Fig. 9. (a) Hydrogen permeation fluxes through pressure change and (b) Arrhenius's plots of the hydrogen permeability on YCC/10wt% Ni membrane.

3.3 Hydrogen Permeance of $Ce_{0.8}Y_{0.2}O_{1.9}$/SiC Membrane

Fig. 10 showed the XRD patterns of the $Ce_{0.8}Y_{0.2}O_{1.9}$ powder. The single phase of $Ce_{0.8}Y_{0.2}O_{1.9}$ (cubic, SG=fm-3m) powder was started to show up at 773 K and progressively enhanced with increasing calcination temperature up to 1473 K. Fig. 11 showed FE-SEM and BET results of the $Ce_{0.8}Y_{0.2}O_{1.9}$ powder. The shape of the powder was a round as modified with oxalic acid as reported before [24]. Oxalic acid could form a mixed precursor, which acts as a substrate for the homogeneous distribution of the mixed metal oxide phases [17].

The morphology and surface area of the SiC ceramic membrane and $Ce_{0.8}Y_{0.2}O_{1.9}$/SiC composite membrane are shown in Fig. 12. The particle size of $Ce_{0.8}Y_{0.2}O_{1.9}$/SiC composite membrane is small and homogeneously distributed among the SiC membrane. It was observed as a slight growth in specific surface area for the case of the composite membrane. The boundaries of SiC grains in this composite membrane are clearer than SiC membrane, as exhibited in Fig. 12 (b). Also, the value of specific surface area (of 56.5 m^2/g) in the composite membrane is bigger than that (of 0.69 m^2/g) in the SiC membrane. From the BET results in Fig. 13, the average pore diameter (25.9 nm) in this membrane was smaller and more concentrated than those in SiC ceramic membrane (31.6 nm).

Fig. 14 showed the XRD profiles of $Ce_{0.8}Y_{0.2}O_{1.9}$/SiC composite membrane before and after hydrogen permeation test. The position of peaks was not changed but the intensity was changed.

In the Rietveld analysis of these results before the test, the ratio of $Ce_{0.8}Y_{0.2}O_{1.9}$, α-phase of SiC-6H and β-phase of SiC-3C was 0.65 %, 51.47 % and 47.88 %, respectively. The remained Si in the SiC ceramic powder seemed to be transformed to β phase (SiC-3C) of SiC after the membrane formation with heat-treatments. Also, the phase transition proceeded from β-(SiC-3C) to α phase (SiC-6H) during heat-treatments. As the results, the amounts of $Ce_{0.8}Y_{0.2}O_{1.9}$, SiC-6H and SiC-3C were changed to 0.54%, 71.83 % and 27.62% after hydrogen permeation test. The stable form of α phase (SiC-6H) was remarkably increased from β phase while the oxide was slightly reduced.

Fig. 15 was a graph for the results of the thermal diffusivity and hydrogen permeance test. Large amount addition of these metal oxides led to the degradation of high-temperature stability of SiC ceramics and mismatch between two phases during fabrication of membrane due to different thermal expansion coefficient. Thus, 1% of $Ce_{0.8}Y_{0.2}O_{1.9}$ mixed oxide was added to SiC ceramic to optimize the microstructure of dense, defect-free SiC-based membrane. The values of thermal diffusivity and the tendency of hydrogen permeance of this membrane were decreased with increasing temperatures. This reduced tendency of the thermal diffusivity was because of phonon scattering effect caused by induced lattice defects on the composite membrane with increasing temperatures [25]. The porosity of the membrane was controlled from 27.3 % (only from SiC membrane) to 23.4 % ($Ce_{0.8}Y_{0.2}O_{1.9}$/SiC composite membrane) as adding complex oxide, $Ce_{0.8}Y_{0.2}O_{1.9}$ powder. The

hydrogen permeation flux of SiC ceramic membrane was large enough to measure and just passed through since the porosity of this membrane was big for the tests. This value on the $Ce_{0.8}Y_{0.2}O_{1.9}$/SiC composite membrane was reduced as 23.4% and the rate of the permeance was measured and calculated as shown in Fig. 15. The hydrogen permeance of this membrane was obtained as $1.07X10^{-5}$ mol/m^2sPa at 373 K. This value was bigger than the value for SiC-based Al_2O_3 ceramic membrane with polystyrene which was reported by H. Suda et al. as $0.3X10^{-7}$ mol/m^2sPa at 373 K. Also, SiO_2 ceramic membrane was by B. K. Sea et al. was $0.2X10^{-7}$ mol/m^2sPa [34-36]. The type of this synthesized membrane is followed by typical Knudsen diffusion mechanism that the value of the permeation flux, permeability, were decreased with increasing the temperatures. This is because the pore size and shape have a significant influence on heat-treatments by ceramic membrane.

To optimize the microstructure of the SiC-based membrane, 1% of $Ce_{0.8}Y_{0.2}O_{1.9}$ metal oxide addition to SiC membrane could be achieved by controlling pore size and distribution, porosity and improved specific surface area. For use as an environmental-friendly a gas filter and support membrane, SiC ceramic membrane should be porous, with a uniform size and pore distribution. Moreover waste SiC sludge could be reused by purifying with several steps and recycle this waste with sintering metal oxide additive to produce the composite membrane as a support for gas filter.

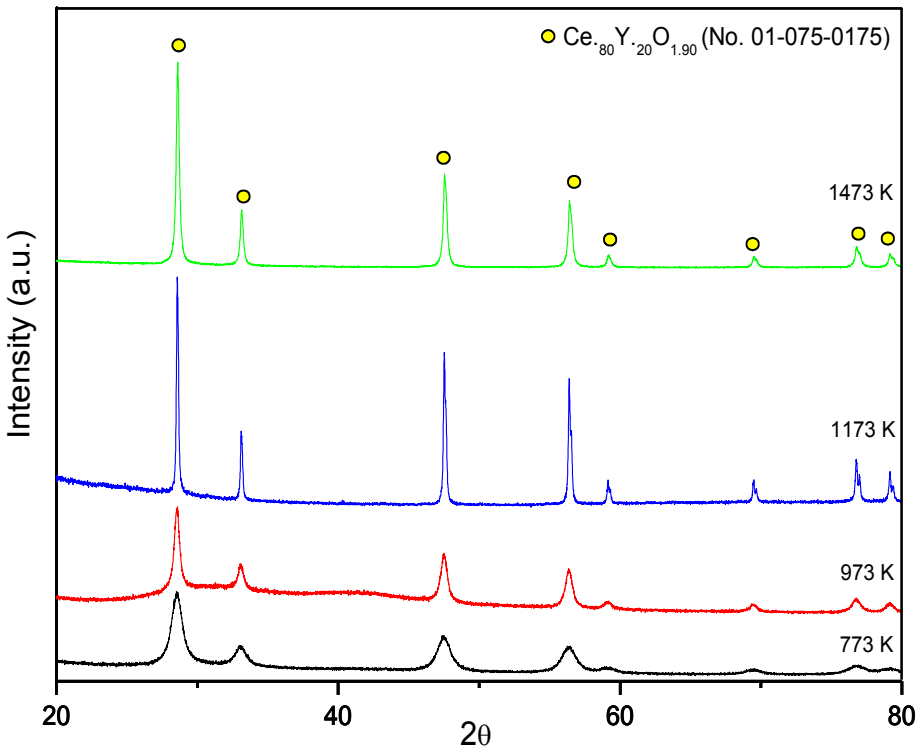

Fig. 10. X-ray diffraction pattern of $Ce_{0.8}Y_{0.2}O_{1.9}$ powder heat-treated at various temperatures under air condition.

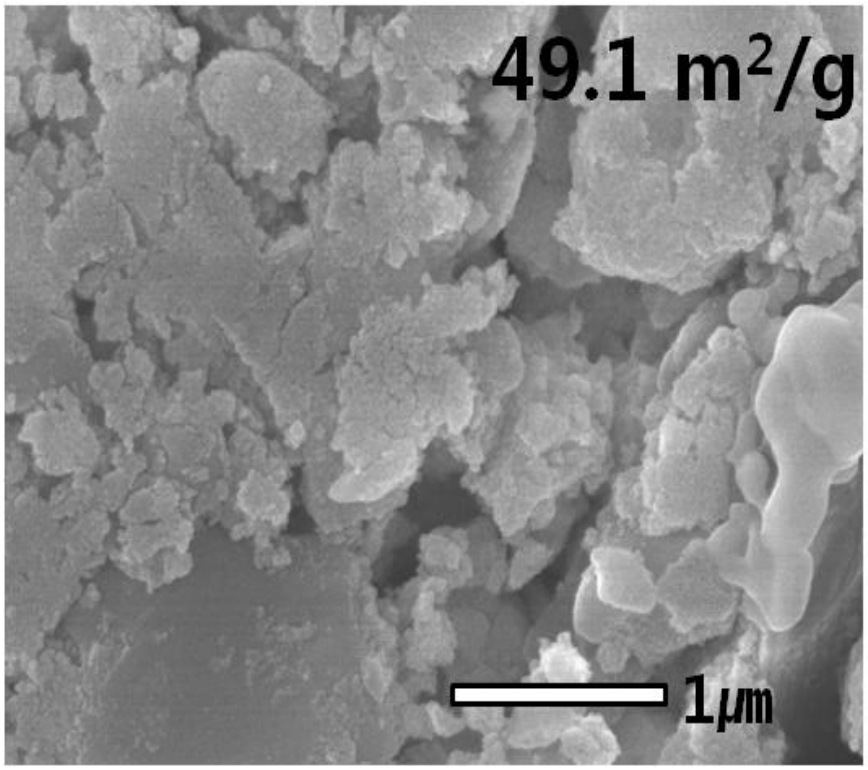

Fig. 11. The surface morphology and surface area of $Ce_{0.8}Y_{0.2}O_{1.9}$ powder heat-treated at 1173K.

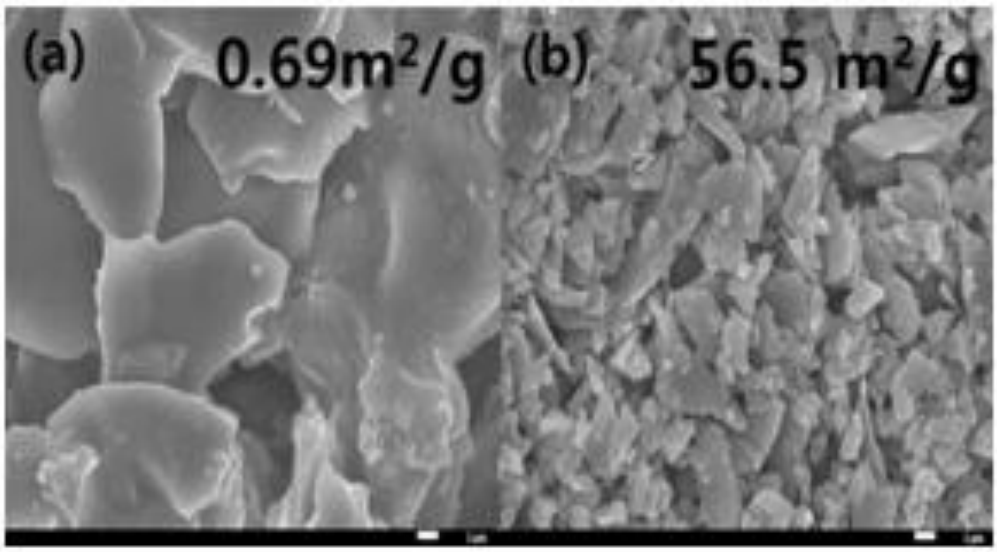

Fig. 12. The FE-SEM pictures and specific surface areas of (a) SiC membrane and (b) $Ce_{0.8}Y_{0.2}O_{1.9}$/SiC composite membrane heat-treated at 1173 K.

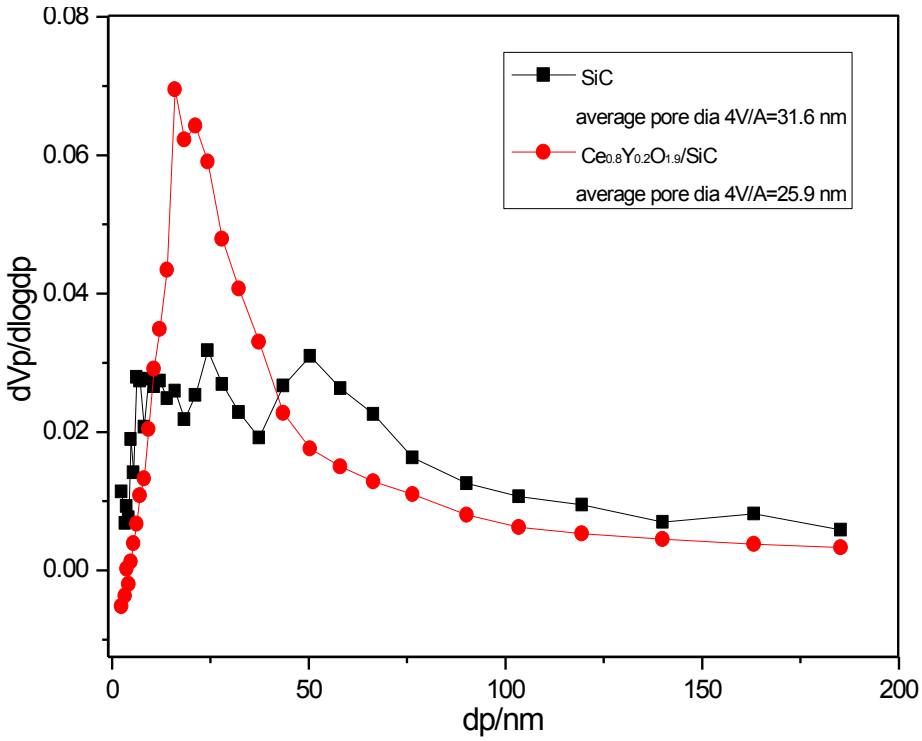

Fig. 13. Pore sizes of $Ce_{0.8}Y_{0.2}O_{1.9}$ oxide powder and $Ce_{0.8}Y_{0.2}O_{1.9}$/SiC composite membrane by BJH method.

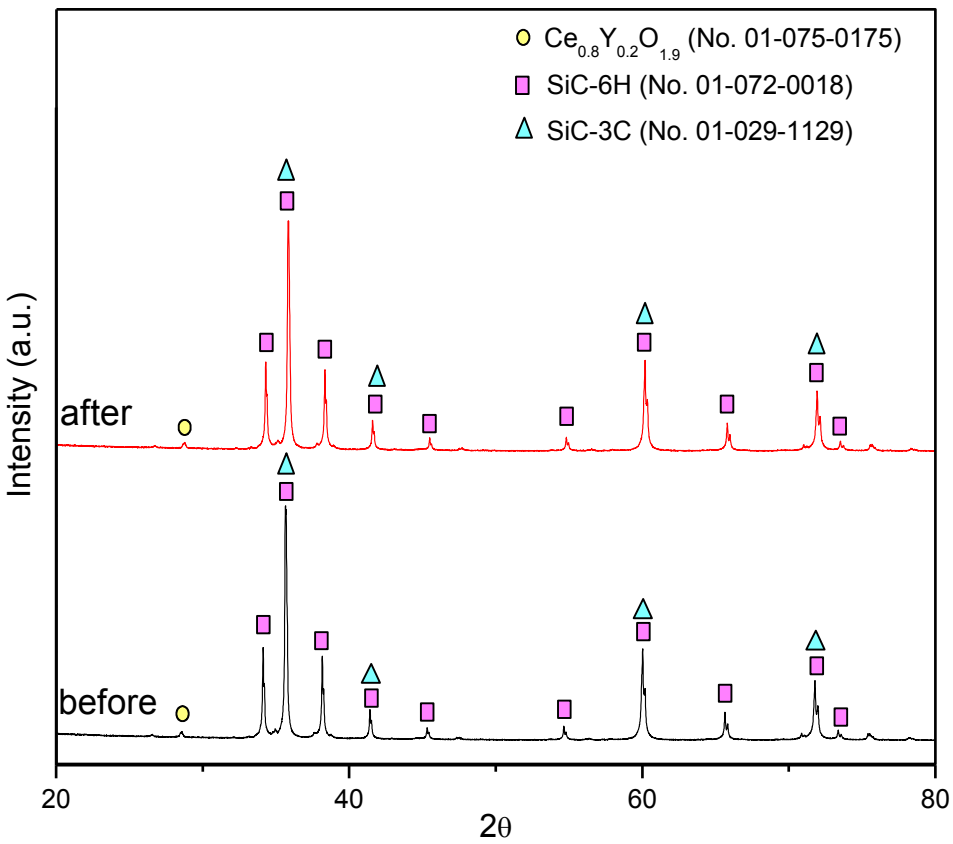

Fig. 14. XRD patterns of $Ce_{0.8}Y_{0.2}O_{1.9}$/SiC composite membrane before and after hydrogen permeation test.

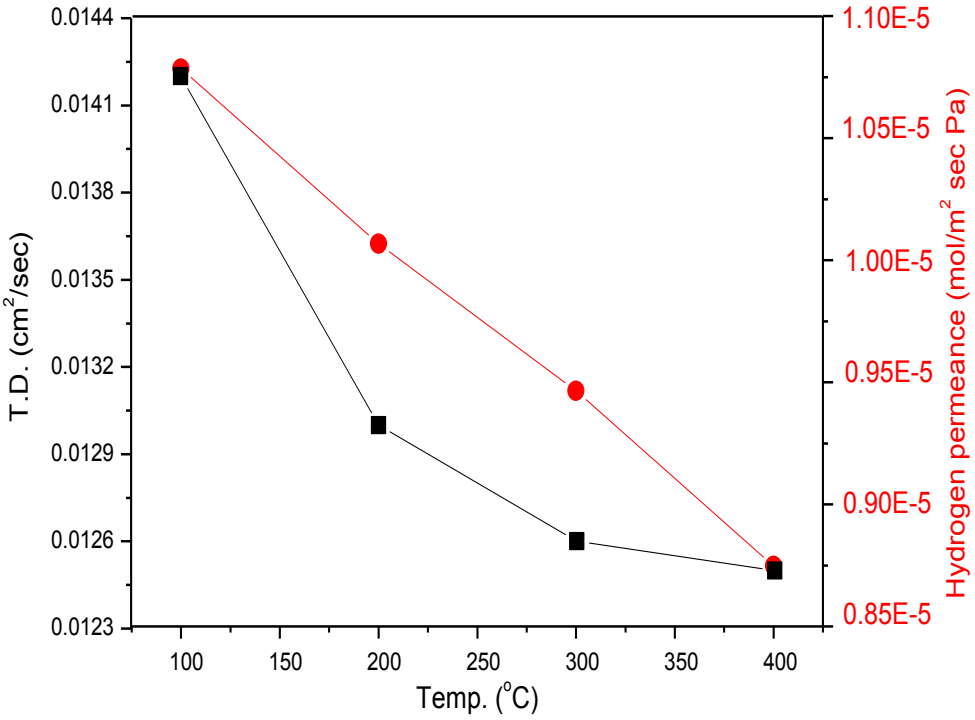

Fig. 15. The thermal diffusivity and hydrogen permeation test with increasing temperatures.

3.4 Hydrogen permeance test of SiC according to amount of Y_2O_3 composite membrane

The XRD pattern of SiC and Y_2O_3 composite membranes with different Y_2O_3 content and then the dip-coated was shown in Fig. 16. The amount of prepared SiC powder was 59.40 % α-phase of SiC-6H, 35.1 % β-phase of SiC-3C and 4.5 % Si phase. After dip-coating, there was no observable change in XRD pattern, but it causes to increase content of Y_2O_3 (cubic, a=1.06 nm, la-3).

Fig. 17 (a) indicated the pore size distribution of SiC+Y_2O_3 composite membranes heat-treated at 1173 K by the BJH (Barrett-Joyner-Halenda) method. Fig. 17 (b) also showed nitrogen sorption isotherms heat-treated at 1173 K. Comparing samples, the composite membrane with the more Y_2O_3 powder had the more uniform pore size distribution and the higher total pore volume. In case of Y_2O_3 30w%, the pore diameter was also the smallest, with a value of 2.4 nm. Two of the membranes, Y_2O_3 10 wt% and 30 wt%, were mesoporous and had an *S*-shaped structure. On the other hand, SiC+Y_2O_3 1 wt% membrane was microporous type. Analyzing these diagrams in both cases, all of the membranes with Y_2O_3 10 and 30 wt% gave rise to a typical type Ⅳ and a membrane with Y_2O_3 1 wt% had Ⅰ type N_2 hysteresis loop, as defined by IUPAC (International Union of Pure and Applied Chemistry). These types of H_2 hysteresis loop were commonly associated with slit pores or voids between close-packed spherical particles of the types.

Fig. 18 showed the surface morphologies of the SiC+Y_2O_3 1, 10 and 30 wt% composite membranes. It was noticeable the agglomerate and small Y_2O_3 particles as increasing the content of Y_2O_3. The coated Y_2O_3 on 1 and 1 wt% Y_2O_3 of SiC composite membranes are shown in Fig. 19.

The results of hydrogen permeance test and selectivity set against CO flux are displayed in Fig. 20. The hydrogen permeance tendency of these membranes was decreased with increasing temperatures. The permeance follows a $(1/T)^{0.5}$ dependence on temperature, indicative of Knudsen-type of transport. This is because the pore size and shape of ceramic membrane are affected significantly by heat-treatment. It was decreased not only the permeance value of hydrogen but also permeance of CO gas as increasing Y_2O_3 content. The permeance of hydrogen of SiC+Y_2O_3 1, 10 and 30 wt% were measured $1.2X10^{-5}$, $8.9X10^{-6}$ and $7.9X10^{-6}$ mol/m^2 s Pa under 298K, respectively. The fig. 20 (b) showed the Arrhenius' s plot for hydrogen permeance data. The calculated data of heat of the process ($\triangle H^o$) for SiC+Y_2O_3 1, 10 and 30 wt% membrane were 1.58, 1.41 and 1.33 J/mol, respectively. This result showed that hydrogen permeance through membrane were measured with the exothermic reaction and dominated by temperature. The activation energy was decreased with adding more Y_2O_3 content. The porosity of the membrane was controlled from 39 % (SiC+Y_2O_3 1 wt% membrane) to 29 % (SiC+Y_2O_3 10 wt% membrane) and 25 % (SiC+Y_2O_3 30 wt% membrane) as adding inorganic oxide. The hydrogen permeation flux of SiC ceramic

membrane was too large to measure and just passed through since the porosity of this membrane was big for the tests.

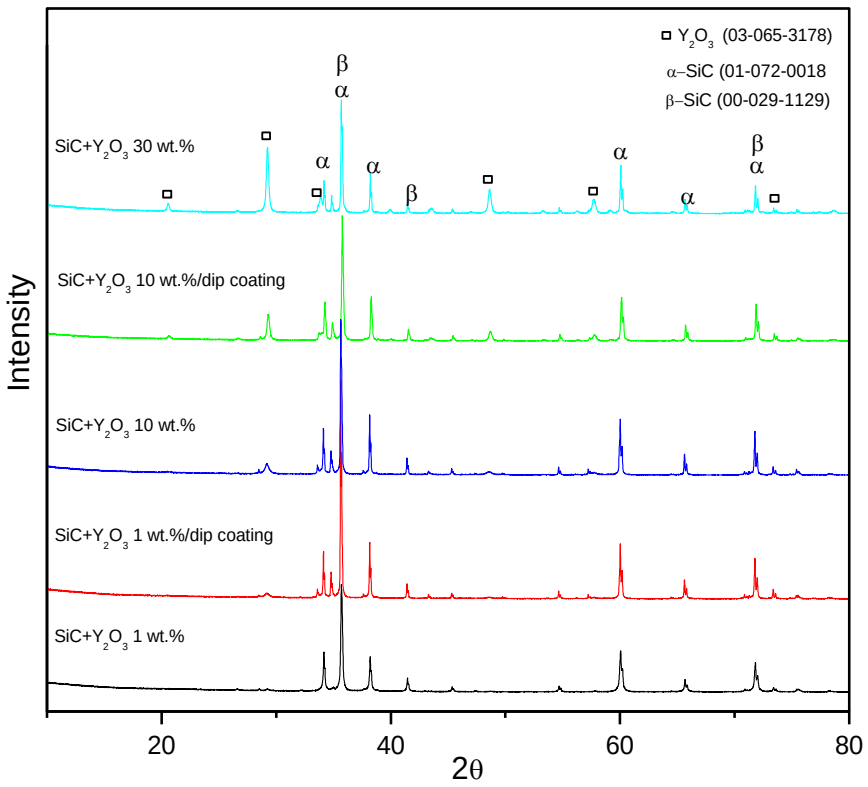

Fig. 16. XRD patterns of SiC+ Y_2O_3 1, 10, 30 wt% composite membranes and dip-coated membranes.

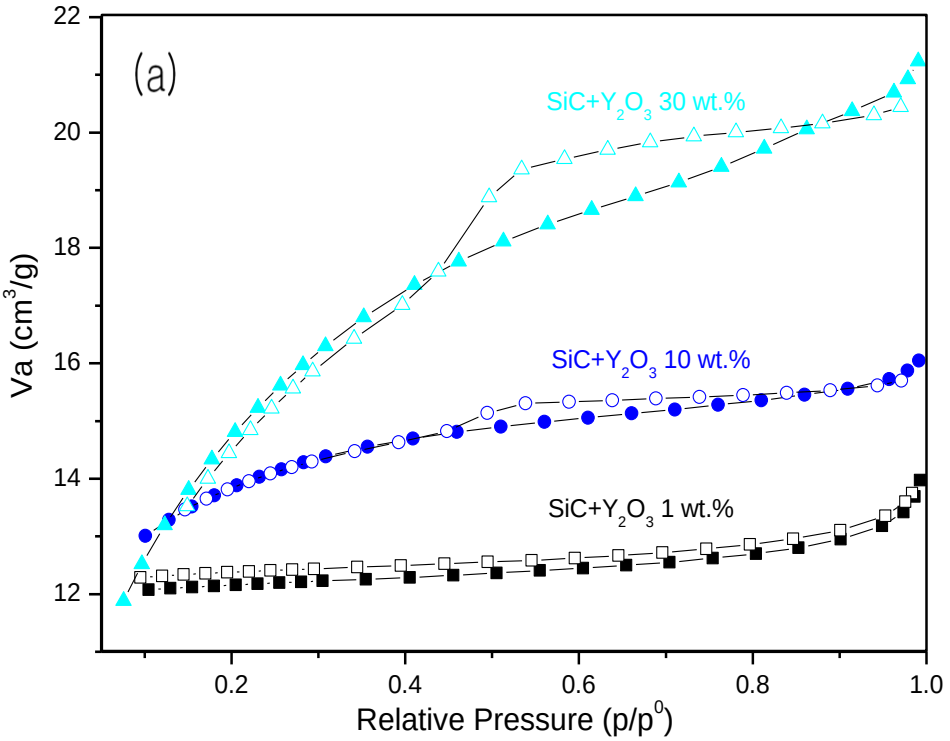
(a)
SiC+Y2O3 30 wt.%
SiC+Y2O3 10 wt.%
SiC+Y2O3 1 wt.%
Va (cm3/g)
Relative Pressure (p/p0)
22
20
18
16
14
12
0.2
0.4
0.6
0.8
1.0

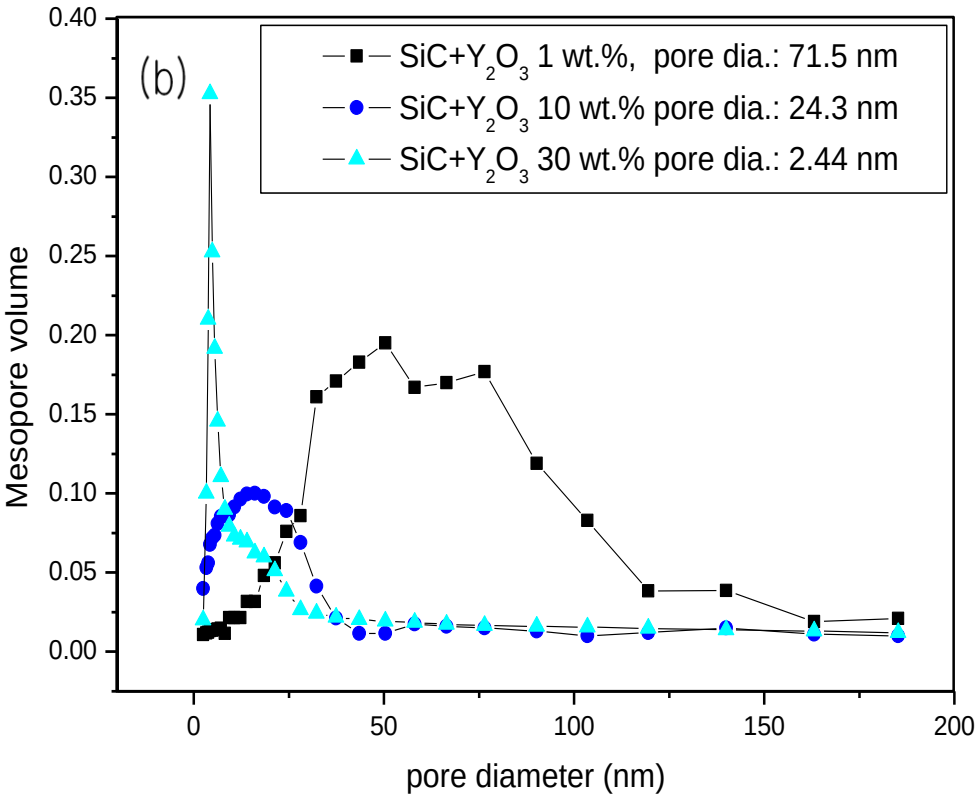

Fig. 17. (a) nitrogen adsorption-desorption isotherms and (b) Pore size distribution of the $SiC+Y_2O_3$ 1, 10, 30 wt% composite membranes heat-treated at 1173 K.

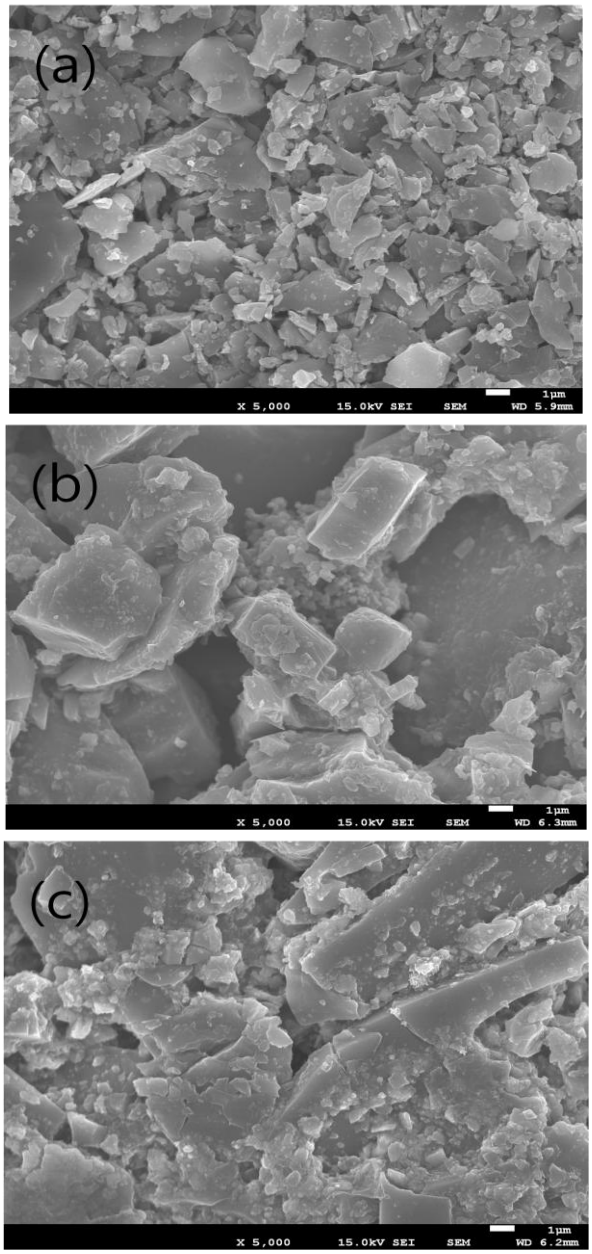

Fig. 18. The surface morphology of (a) SiC+ Y_2O_3 1 wt%, (b) Y2O3 10 wt% and (c) Y_2O_3 30 wt% composite membranes heat-treated at 1173K.

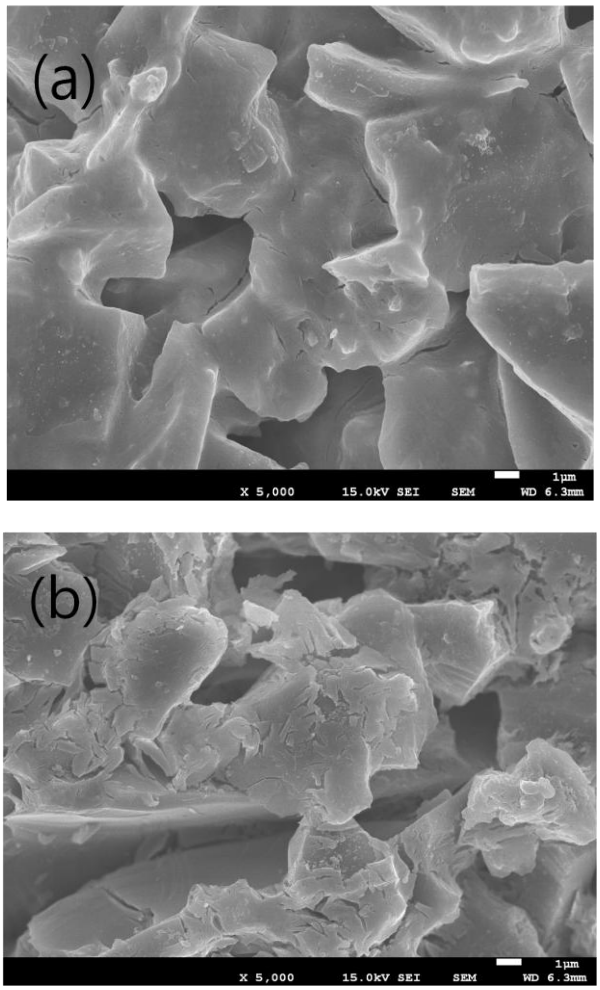

Fig. 19. The surface morphology of (a) SiC+Y_2O_3 1 wt% and, (b) Y_2O_3 10 wt% composite membranes using dip-coating.

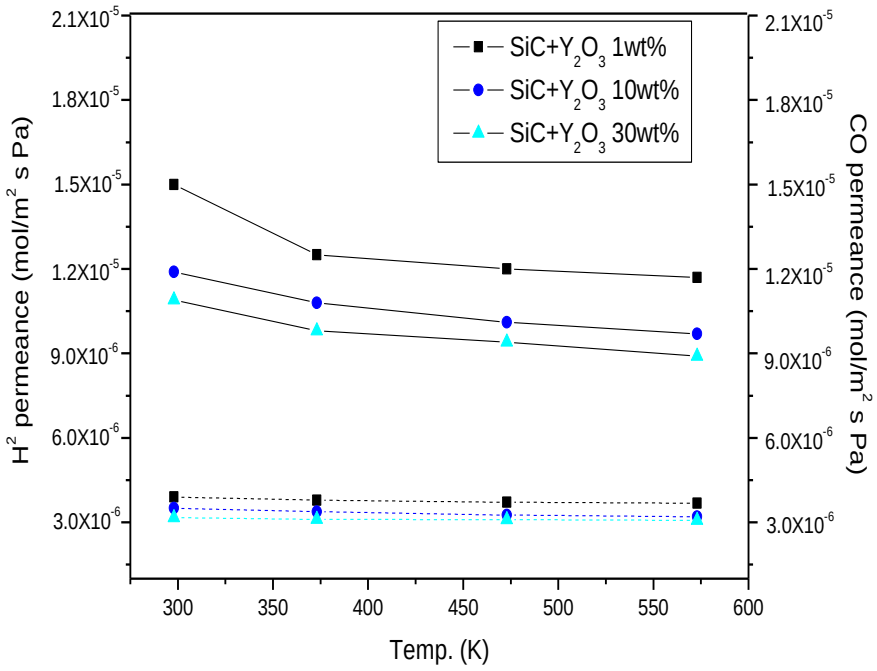

Fig. 20. (a) The hydrogen and carbon monoxide permeation tests of SiC+ Y_2O_3 1, 10, 30 wt% composite membranes with increasing temperatures.

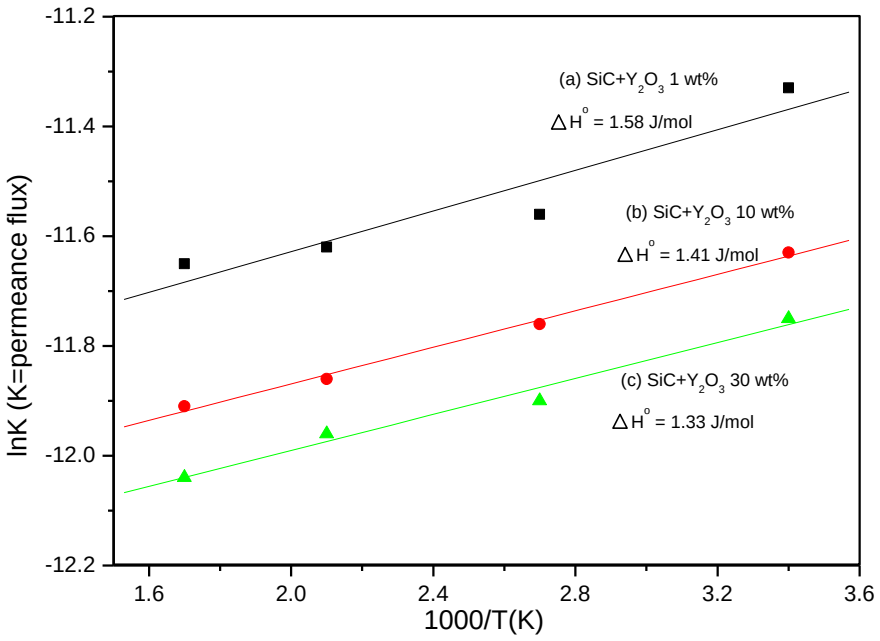

Fig. 20. (b) Arrhenius' s plots of the hydrogen permeance on SiC+ Y_2O_3 1, 10, 30 wt% composite membranes.

Table.1. The porosity of SiC+Y_2O_3 1, 10, 30 wt% and membranes using dip-coating.

Sample	Porosity
SiC+Y_2O_3 1%	39 %
SiC+Y_2O_3 10%	29 %
SiC+Y_2O_3 30%	25 %
SiC+Y_2O_3 1%/dip-coating	32 %
SiC+Y_2O_3 10%/dip-coating	24 %
SiC+Y_2O_3 30%/dip-coating	22%

Ⅳ. Conclusion

This work was conducted to investigate the hydrogen permeation of cermets, 20 wt.% NiO-doped Al_2O_3/10 wt.% Ni and YCC/10 wt.% Ni, and ceramic membranes, SiC+$Ce_{0.8}Y_{0.2}O_{1.9}$ and SiC+Y_2O_3, under increasing pressure or temperature.

At first, the NiO-doped Al_2O_3 powder synthesized by sol-gel method was useful for ceramic supports because it had high specific surface area and enhanced thermal stability at high temperature. The 20 wt.% NiO-doped Al_2O_3/10 wt.% Ni composite materials were prepared successfully by the HPS process and obtained as an excellent membrane with high hydrogen permeability about 0.1 mol/m^2s at 673 K.

The Y_2O_3-based composite powder was controlled surface morphology by adding oxalic acid. Oxalic acid was effective on controlling shape of the particle and leads to increase the specific surface area. The hydrogen flux of YCC/Ni composite membrane was obtained as 7.7x10^{-7} mol/m^2s at 573 K under 0.2 MPa. It was better than for the Pd/YSZ membrane (4.3x10^{-7} mol/m^2s at 873 K). The hydrogen flux increased with increasing pressure but was not correlated with temperature. The membrane has Knudsen diffusion mechanism that is not proportional the increasing temperature and hydrogen pressure.

SiC was considered as a membrane support to improve weak durability of cermet. SiC has advantages such as excellence of thermal shock with corrosion resistance at elevated temperatures as well as having low coefficient of thermal expansion and high

mechanical strength. However SiC has a disadvantage, porous. The porosity of the membrane was controlled and reduced from 27.3 % (only from SiC) to 23.4 % ($Ce_{0.8}Y_{0.2}O_{1.9}$/SiC composite) as adding complex oxide, $Ce_{0.8}Y_{0.2}O_{1.9}$ powder to SiC ceramic membrane. The 1% of $Ce_{0.8}Y_{0.2}O_{1.9}$ powder was distributed homogeneously into the SiC membrane by analyzing the FE-SEM results. The average pore diameter and distribution of composite membrane was smaller and more uniform than those of SiC ceramic membrane, respectively. The $Ce_{0.8}Y_{0.2}O_{1.9}$/SiC sample had thermal diffusivity of $1.6X10^{-2}$ cm^2/s at 298K. The values of thermal diffusivity and the tendency of hydrogen permeance of this membrane were decreased with increasing temperatures. The hydrogen permeance of this composite membrane was obtained as $1.07X10^{-5}$ mol/m^2sPa at 373 K. This value was bigger than SiO_2 ceramic membrane as reported B. K. Sea et al. ($0.2X10^{-7}$ mol/m^2sPa) [34].

The prepared disc membranes passed through dip-coating process with Y_2O_3 sol solution to more reduce porosity of SiC. SiC+Y_2O_3 1 wt.%, 10 wt.% and 30 wt.% reduced the porosity by dip-coating process from 39%, 29% and 25% to 32%, 24% and 22%, respectively. It is not only decreased the permeance value of hydrogen but also permeance of CO gas as increasing Y_2O_3 content. The permeances of hydrogen of SiC+Y_2O_3 1, 10 and 30 wt% were measured $1.2X10^{-5}$, $8.9X10^{-6}$ and $7.9X10^{-6}$ mol/m^2 s Pa under 298K, respectively.

I studied inorganic composite materials such as NiO-doped

Al_2O_3/Ni, YCC/Ni, $Ce_{0.8}Y_{0.2}O_{1.9}$/SiC and Y_2O_3/SiC in an attempt to have high hydrogen permeation. From these results, I proposed that hydrogen permeation was only improved without any effects of diffusion mechanism. Also the durability of membranes is enhanced far and away the best as using SiC.

Reference

[1] S. Sircar and T. C. Golden; Purification of Hydrogen by Pressure Swing Adsorption, Separ. Sci. Technol. 35 (5), 667-687, 2000

[2] U. Balachandran, T. H. Lee, L. Chen, S. J. Song, J. J. Picciolo and S. E. Dorris; Hydrogen separation by dense cermet membranes, Fuel, 85, 150- , 2006

[3] S. Adhikari and S. Fernando; Hydrogen Membrane Separation Techniques, Ind. Eng. Chem. Res., 45 (3), 875-881, 2006

[4] Z. Zhu, W. Sun, L. Yan, W. Liu and W. Liu; Synthesis and hydrogen permeation of Ni-Ba(Zr0.1Ce0.7Y0.2)O3-δ metla-ceramic asymmetric membranes, Int. J. Hydrogen Energy, 36, 6337-6342, 2011

[5] M. G. Ma and J. F. Zhu; A Facile Solvothermal Route to Synthesis of γ-Alumina with Bundle-like and Flower-like Morphologies, Mater. Lett., 63, 881-883, 2009

[6] K. Y. Lim, Y. W. Kim, I. H. Song, H. D. Kim, and J. S. Bae; Effect of First Content on Microstructure and Flexural Strength of Porous First-Bonded Al_2O_3 Ceramics(in Korean), J. Kor. Ceram. Soc., 47 (6]), 529-533, 2010

[7] A. Pokhrel, J. G. Parks, G. H. Jho, J. Y. Kim, and I. J. Kim; Controlling the Porosity of Particle Stabilized Al_2O_3 Based Ceramics, J. Kor. Ceram. Soc., 48 (6), 600-603, 2011

[8] A. Nandi, M. D. Gupta and A. K. Banthia; Sulfonated Polybutadiene Ionomer Templates Nanonickel Composite, Mater. Lett., 52, 203-205, 2002

[9] Z. Jun, S. J. Wang, and X. H. Luo; Dispersion of Nanonickel into γ-Al_2O_3 Studied by Positron, Radiat. Phys. Chem., 68, 541-544, 2003

[10] J. Li, X. Wang, L. Wang, Y. Hao, Y. Huang, Ye. Zang, X. Sun and X. Liu: Preparation of alumina membrane from aluminium chloride, 275 (1-2), 6-11, 2006

[11] F. Huang, Y. Zheng, G. Cai, Y. Zheng, Y. Xiao and K. Wei: A new synthetic procedure for ordered mesoporous γ-alumina with a large surface area, Scripta Materialia, 63 (3), 339-342, 2010

[12] H. Xu, H. Yan and Z. Chen; Sintering and Electrical Properties of Ce0.8Y0.2O1.9 powders Prepared by Citric Acid-Nitrate Low-temperature Combustion process, J. Power Sources, 163 (1), 409-414, 2006

[13] M. Kodo, K. Soga, H. Yoshida and T. Yamamoto; Doping effect of divalent cations on sintering of polycrystalline yttria, J. Eur Ceram. Soc., 30, 2741-2747, 2010

[14] W. Yao, G. Z. Lu, Y. L. Guo, Y. Guo, Y. Q. Wang and Z. G. Zhang; Promotional effect of Y2O3 on the performance of Ag/a-Al2O3 catalyst for epoxidationof propylene with molecular oxygen, J. Mol. Catal. A Chem., 276, 162-167, 2007

[15] S. H. Kenawy and W. M. N. Nour; Microstructural evaluation of thermally ratigued SiC-reinforced Al_2O_3/ZrO_2 matrix composites, J. Mater. Sci, 40, 3789-3793

[16] T. Talebi, M. H. Sarrafi, M. Haji, B. Raissi and A. Maghsoudipour: Investigation on microstructures of NiO-YSZ composite and Ni-YSZ cermet for SOFCs, Int. J. Hydrogen Energy,

35 (17), 9440-9447, 2010
[17] T. M. Adams and J. Mickalonis: Hydrogen permeability of multiphase V-Ti-Ni metallic membrnaes, Mater. Lett., 61 (3), 817-820, 2007
[18] A. L. Ahmad and N. N. N. Mustafa: Sol-gel synthesized of nanocomposite palladium-alumina ceramic membrane for H_2 permeability: Preparation and charaterization, Int. J. Hudrogen Energy, 32 (12), 2010-2021, 2007
[19] N. Srisiriwat, S. Therdthianwong and A. Therdthianwong: Oxidative steam reforming of ethanol over Ni/Al_2O_3 catalysts promoted by CeO_2, ZrO_2 and CeO_2-ZrO_2, Int. J. Hydrogen Energy, 34 (5), 2224-2234, 2009
[20] J. H. Park, T. W. Hong and M. W. Jung: Hydrogen permeation on Al_2O_3-based nickel/cobalt composite membranes, Int. J. Hudrogen Energy, 35 (23), 12976-12980, 2010
[21] B. Ernst, S. Haag and M. Burgard: Permselectivity of a nickel/ceramic composite membrane at elevated temperatures: A new prospect in hydrogen separation, J. Membr. Sci., 288 (1-2), 208-217, 2007
[22] L. Yan, W. Sun, L. Bi, S. Fang, Z. Tao and W. Liu: Influence of fabrication process of $Ni-BaCe_{0.7}Zr_{0.1}Y_{0.2}O_{3-\delta}$ cermet on the hydrogen permeation performance, J. Alloys Compd., 508 (1), L5-L8, 2010
[23] M. Rezaei, M. Khajenoori, and B. Nematollahi; Synthesis of High Surface Area Nanocrystalline MgO by Pluronic P123 Triblock copolymer Surfactant, Powder Technol., 205, 112-216,

2011
[24] Q. Wu, W. Li, Y. Cheng, and Z. Jiang; Homogenous $LiCoO_2$ Nanoparticles Prepared Using Surfactant P123 as Templatem and its Application to Manufacturing Ultra-thin-film Electrode, Mater. Chem. Phys., 91, 463-467, 2005
[25] C. H. Wang, S. S. Lin, C. L. Chen, and H. S. Weng; Performance of the Supported Copper Oxide Catalysts for the Catalytic Incineration of Aromatic Hydrocarbons, Chemosphere, 64, 503-509, 2006
[26] M. Akia, S. M. Alavi, M. Rezaei, and Z. F. Yan; Optimising the Sol-gel Parameters on the Synthesis of Mesostructure Nanocrystalline γ-Al_2O_3, Micropor. Mesopor. Mater., 122, 72-78, 2009
[27] G. Stoica, M. Santiago, P. A. Jacobs, J. Perez-Ramirez, and P. P. Pescarmona; Epoxidation Catalysts Derived from Aluminium and Gallium Dawsonites, Appl. Catal. A, 371, 43-53, 2009.
[28] L. S. Sigl and H. J. Kleebe; Core/Rim Structure of Liquid-phase-sintered Silicon Carbide, J. Am. Ceram. Soc., 76 (3), 773-776, 1993
[29] S. Zhu, S. Ding, H. Xi and R. Wang; Low-temperature fabrication of porous SiC ceramics by preceramic polymer reation bonding, Mater. Lett. 59 (5), 595-597, 2005
[30] C. Kleinlogel and L. J. Gauckler; Sintering of Nanocrystalline CeO_2 Ceramics, Adv. Mater., 13 (14), 1081-1085, 2001
[31] M. Ge, C. Guo, L. Li, B. Zhang, Y. Feng and Y. Wang;

Preparation of CeO_2 novel sponge-like rods by emulsion liquid Membrane System and its Catalytic Oxidation Property, Mater. Lett., 63 (15), 1269-1271, 2009

[32] F. Y. Wang, S. Chen and S. Cheng; Gd^{3+} and Sm^{3+} Co-doped Ceria Based Electrolytes for Intermediate Temperature Solid Oxide Fuel Cells, Electrochem. Commun. 6 (8), 743-872, 2004

[33] B. Y. Shon, T. W. Hong and M. W. Jung; Hydrogen permeation of Y_2O_3-CuO-CeO_2/Ni composite membrane, Solid State Ionics, 225, 695-698, 2012

[34] H. Inaba and H. Tgawa; Ceria-based solid electrolytes, Solid State Ionics, 83 (1-2), 1-16, 1996

[35] H. Lim, Y. Gu and S. T. Oyama; Studies of the effect of pressure and hydrogen permeance on the ethanol steam reforming reaction with palladium and silica-based membranes, J. Membr. Sci., 396, 119-127, 2012

[36] B. K. Sea, K. Ando, K. Kusakabe and S. Morooka; Separation of hydrogen from steam using a SiC-based membrane formed by chemical vapor deposition of triisopropylsilane, J. Membr. Sci., 146, 73-82, 1998

[37] Y. L. Yun and W. H. Ju, Chem. Ind. Technol., 16(2), 98 (1998)

[38] K. Y. Hwang, H. C.Ko and T. W. Yeu; Preparation of a microporous silica power by sol-gel process, J. Korean Ind. Eng. Chem, 11 (5), 495-499, 2000

[39] Y. H. Deng, C. C. Wang, J. H. Hu, W. L. Yang and S. K. Fu, Colloids Surf. A, 26, 87 (2005)

[40] A. Dupont, C. Parent, B. Le Garrec and J. M. Heintz, J. Solid

State Chem., 171, 152 (2003)
[41] M. P. Pileni, J. Phys. Chem. B, 105, 3358 (2001)
[42] K. Khoabane, E. M. Mokoena and N. J. Covile, Micropor. Mesopor. Mater., 83, 67 (2005)
[43] T. Kumagai, H. Yokota, K. Kawaguchi, W. Kondo, S. Mizuta; Preparation of superconducting $YBa_2Cu_3O_{7-8}$ thin films by the dipping-pyrolysis process using organic acid salts, Chem. Lett. 16 1645-1646, 1987
[44] A. Ueno, H. suzuki, Y. Kotera; Particle-size distribution of nickel dispersed on silica and its effects on hydrogenation of propionaldehyde, J. Chem. Soc. Faraday Trans., 79 127-136, 1983
[45] A. Raveh, Z. K. Tsameret, E. Grossman; Surface characterization of thin layers of aluminium oxide, Surface and Coatings Technology, 88, 103-111, 1996
[46] C. Bousquet, C. Elissalde, C. Aymonier, M Maglione, F Cansell, J.M. Heintz; Tuning Al_2O_3 crystallinity under supercritical fluid conditions: Effect on sintering, Journal of the European Ceramic Society, 28, 223-228, 2008
[47] J. A. Wang, X. Bokhimi, A. Morales, O. Novaro; Aluminum Local Environment and Defects in the Crystalline Structure of Sol-Gel Alumina Catalyst, J. Phys. Chem,. B103, 299-303, 1999
[48] A. K. Prabhu and S. T. Oyama; Highly hydrogen selective ceramic memnbranes: application to the transformation of

greenhouse gases, J. Membr. Sci. 176, 233-248, 2000
[49] S. Fang, L.Bi, L. Yan, W. Sun, C. Chen and W. Liu; CO2-Resistant Hydrogen Permeation Membrane Based on Doped Ceria and Nickel, J. Phys. Chem. C, 114, 10986-10991, 2010
[50] H. R. Lee, B. K. Seo and Y. J. Choi; Control of Nano-structure of Ceramic Membrane and Its Application, J. Membr. Sci, 22 (2), 77-94, 2012

Abstract

Synthesis and Evaluations of Hydrogen Permeations on Al_2O_3, Y_2O_3 based Inorganic Composite Materials

Bo young Son
Department of Chemistry
Graduate School of
Sungshin Women's University

Hydrogen has attracted clean energy media as high-quality and renewed energy source in recent years. On the one hand, a ceramic catalyst and/or catalyst support such as Al_2O_3, Y_2O_3 has often preferred choice due to their specific properties such as thermal stability and high surface area. The nanoporous hydrogen selective SiC membrane has been used for application in membrane reactors for the water gas shift and steam reforming reactions. Silicon carbide (SiC) has been used as a structural material because of its excellent of thermal shock and corrosion resistance at elevated temperatures. Due to these advantages, SiC is also available for gas and liquid separation filter material. The metal oxides such as Al_2O_3, Y_2O_3 and CeO_2 are commonly combined as inorganic additives for densification of SiC ceramic materials. The characterizations of the synthesized powders and composige membranes were measured TG-DTA, XRD, BET and FE-SEM. Hydrogen permeation evaluations were examined at various temperatures under increasing pressure.